TOP-DOWN EFFECTS OF ATTENTION ON THE ACTION OBSERVATION NETWORK

A THESIS SUBMITTED TO
THE GRADUATE SCHOOL OF ENGINEERING AND SCIENCE
OF BILKENT UNIVERSITY
IN PARTIAL FULFILLMENT OF THE REQUIREMENTS FOR
THE DEGREE OF
MASTER OF SCIENCE
IN
NEUROSCIENCE

By
Aslı Eroğlu
July 2024

Top-down effects of attention on the action observation network
By Aslı Eroğlu
July 2024

We certify that we have read this thesis and that in our opinion it is fully adequate, in scope and in quality, as a thesis for the degree of Master of Science.

Burcu Ayşen Ürgen(Advisor)

Ausaf Ahmed Farooqui

Murat Perit Çakır

Approved for the Graduate School of Engineering and Science:

Orhan Arıkan
Director of the Graduate School

ABSTRACT

TOP-DOWN EFFECTS OF ATTENTION ON THE ACTION OBSERVATION NETWORK

Aslı Eroğlu
M.S. in Neuroscience
Advisor: Burcu Ayşen Ürgen
July 2024

Action perception is one of the fundamental skills for survival and social interaction. In neuroscience literature, it is well-established that when an action is visually perceived, the Action Observation Network (AON) becomes active in the human brain. This network has three core brain regions: the posterior superior temporal sulcus (pSTS), parietal cortex, and premotor cortex. Recent studies in neuroscience have shown that action perception is not a passive process but is affected by top-down signals such as attention. In this study, we investigated the influence of attention on the AON by conducting a two-session fMRI experiment. The stimuli comprised eight videos of pushing actions, with each video featuring a unique combination of actor (female or male), effector (hand or foot), and target (object or human). In the active fMRI session, participants viewed the videos while performing three different tasks that directed their attention to distinct features of the action (actor, effector, target). In the passive fMRI session, participants viewed the same videos without performing any task. The data from the passive session was used to extract ROIs: pSTS, parietal, and premotor in each hemisphere. Univariate analysis, representational similarity analysis (RSA), and decoding analysis were performed. Univariate analysis showed that introducing attentional demands during video viewing elicited a significant increase in neural activity within both parietal and premotor cortices relative to passive viewing conditions. RSA results revealed significant correlations between neural activity patterns and task models across all ROIs, indicating top-down influence throughout the AON. Decoding analysis showed unique top-down effects in each ROI, depending on its hierarchical level and intrinsic selectivity. These findings demonstrate strong top-down modulation of the AON based on cognitive demands, highlighting the dynamic interplay of attention and action perception.

Keywords: action perception, fMRI, attention, top-down modulation, feature-based attention.

ÖZET

YUKARIDAN AŞAĞIYA DİKKAT SÜREÇLERİNİN EYLEM ALGISI AĞI ÜZERİNDE ETKİSİ

Aslı Eroğlu
Nörobilim, Yüksek Lisans
Tez Danışmanı: Burcu Ayşen Ürgen
Temmuz 2024

Eylem algısı, hayatta kalma ve sosyal etkileşim için gerekli olan temel becerilerden biridir. Sinirbilim literatüründen bilindiği üzere bir eylemi görsel olarak algıladığımızda beynimizdeki Eylem Algısı Ağı (EAA) aktif hale gelir. Bu ağdaki üç temel beyin bölgesi posterior superior temporal sulkus (pSTS), parietal korteks ve premotor kortekstir. Sinirbilim alanında yapılan son çalışmalar, eylem algısının pasif bir süreç olmadığını, dikkat gibi yukarıdan aşağıya sinyallerden etkilendiğini göstermiştir. Bu çalışmada, iki oturumluk bir işlevsel manyetik rezonans görüntüleme (iMRG) deneyi yürüterek dikkat süreçlerinin EAA üzerindeki etkisini araştırdık. Uyaranlar, itme eyleminin gösterildiği 8 videodan oluşuyordu ve bu itme eylemi iki farklı aktör tarafından (kadın, erkek) iki farklı uzuv ile (el, ayak) iki farklı hedefe (obje, insan) uygulandı. Birinci iMRG oturumunda, katılımcılar videoları izlerken aynı zamanda dikkatlerini eylemin farklı özelliklerine (aktör, uzuv, hedef) yönlendiren üç farklı görev gerçekleştirdiler. İkinci iMRG oturumunda ise katılımcılar aynı videoları herhangi bir görev yapmadan izlediler. İkinci oturumdan elde edilen veriler, her iki yarım küredeki pSTS, parietal ve premotor bölgeler olmak üzere özel ilgi alanlarının belirlenmesi için kullanıldı. Daha sonra ise tek değişkenli analiz, temsili benzerlik analizi (TBA) ve çok değişkenli sınıflandırma analizi yapıldı. Tek değişkenli analiz sonuçlarıyla birlikte, videoların pasif bir şekilde izlendiği duruma dikkat gibi bilişsel bir süreç eklendiğinde parietal ve premotor bölgelerdeki aktivitenin genişlediğini gözlemledik. TBA sonuçları, nöral aktivite örüntülerinin tüm özel ilgi bölgelerinde görev modeliyle istatistiksel olarak anlamlı bir şekilde ilişkili olduğunu gösterdi. Bu, yukarıdan aşağıya sinyallerin EAA'nın tüm katmanlarını etkilediğini göstermektedir. Çok değişkenli sınıflandırma analizi, hiyerarşik seviyelerine ve içsel seçiciliğine bağlı olarak, özel ilgi alanlarının yukarıdan aşağıya

görevlerle ilişkili sinyallerden benzersiz şekilde etkilendiğini göstermiştir. Bu sonuçlar, EAA'nın bilişsel talebe bağlı olarak önemli ölçüde yukarıdan aşağıya bir şekilde modüle edildiğini göstermekte ve dikkat ile eylem algısı süreçleri arasındaki dinamik etkileşimi vurgulamaktadır.

Anahtar sözcükler: eylem algısı, iMRG, dikkat, yukarıdan aşağıya süreçler, özellik-temelli dikkat.

Acknowledgement

I want to express my sincere gratitude to all who contributed to this thesis and helped me complete this project. Thanks to many great people, my master's journey has become an incredible opportunity for me to learn a lot of things and grow.

First, I would like to thank my beloved advisor, Dr. Burcu Ayşen Ürgen. She always guided me toward becoming a good scientist and inspired me with her enthusiasm and endurance. She was always there for us with her endless understanding, providing guidance and support both inside and outside the lab. I feel lucky to have worked with her, and it was a great pleasure. I will always be grateful to her for trusting me and opening the door to the field of neuroscience for me.

Also I want to thank my jury committee, Dr. Ausaf Ahmed Farooqui and Dr. Murat Perit Çakır, for their time and valuable feedback.

Next, I want to thank my mom, dad, brother, and his dear family for their endless love and support. They always wanted the best for me. It would be nearly impossible to complete this thesis without the motivation they gave me.

And finally, I want to express my deep gratitude to my lovely friends. I am thankful to Rabia, Murat, and Simay for being sincere friends from the beginning and forming many valuable memories, to Aysu for building deep friendships and strengthening the connection between our friend groups, to Şeyda for her friendly and professional support, and to Feza for always being there for me with his kind heart, sharing wisdom on both personal and academic matters. Without the love and support of my friends, it would be a dull and incomplete experience. Also, I am grateful to all my lab mates for valuable scientific discussions and fun lab parties.

Before concluding, I want to thank Turkey's Scientific and Technological Research Council (TÜBİTAK) for making this project possible with a 1002-A (223K918), A Short term Support Module.

Contents

1 Introduction **1**

1.1 Action Perception 1

1.2 Role of Attention in Perception 4

1.3 Previous Research 5

1.4 Current Study 6

2 Methods **8**

2.1 Participants 8

2.2 Stimuli and Experimental Design 8

2.2.1 Stimuli 8

2.2.2 Experimental Design and Setup 9

2.2.3 Data Acquisition 11

2.3 Behavioral Analysis 13

2.4 Univariate Analysis 13

2.5 Representational Similarity Analysis 14

2.6 Decoding Analysis 16

3 Results **18**

3.1 Behavioral Results 18

3.2 Univariate Analysis Results and ROI Selection 19

3.2.1 Data Cleaning 19

3.2.2 Univariate Results 19

3.2.3 Identification of ROIs 24

3.3 Representational Similarity Analysis Results 25

3.4 Decoding Analysis Results 27

4 Discussion **31**

4.1 Discussion of the Results 31

4.2 Conclusion 35

4.3 Limitations 36

4.4 Future Directions 37

A Code **48**

B Permissions **49**

List of Figures

1.1 Meta-analysis results for action observation [1]. pMTG posterior middle temporal gyrus, SMA supplementary motor area; BA 44, 45: Broca's area [2]; BA 6: lateral premotor cortex [3]; SI: primary somatosensory cortex (BA 2 [4]); 7A: superior parietal area [5]; PFt: inferior parietal area [6] [7]; hIP3: intraparietal area [5]; V5: extrastriate visual area [8]. (Reprinted with permission.) 3

1.2 The core brain regions of AON. pSTS: posterior superior temporal sulcus 3

2.1 The stimuli for fMRI experiments: One frame from each video, demonstrating the action with variations in actor, effector, and target. 9

2.2 Experimental design for a set (top) and a block (bottom). The hand figure represents the response interval. ISI: interstimulus interval. 10

2.3 The structure of the model RDMs. Its size is 24x24, representing 8 action videos under 3 different attention tasks 15

2.4 6 model RDMs, to be compared with neural RDMs for each region of interest (ROI). These models represent different aspects: actor, effector, and target models capture video features; the task model represents unique tasks; the visual model reflects visual similarity between videos; and the random model, generated with random numbers, acts as a control model for comparison. 16

3.1 Activation maps resulted from videos minus rest contrast (FWE corrected, $p<0.05$) of passive session (top) and active session (bottom). The white borders show the activation area of the passive session at $p<0.001$ uncorrected level. The visualization was done with Caret5 software. Landmarks are indicated in black: PreSC (Pre-central sulcus), CS (Central sulcus), PostCS (Post-central sulcus), IPS (intra-parietal sulcus), POS (parieto-occipital sulcus), STS (superior temporal sulcus), ITS (inferior temporal sulcus), OTS (occipito-temporal sulcus). 21

3.2 Activation maps of actor task (top), effector task (middle) and target task (bottom). All activation maps were derived from videos and rest contrast for significance level at $p<0.05$ with FWE correction. The white borders are representation of passive session videos and rest condition at significance level at $p<0.001$, uncorrected. . 23

3.3 Visualization of ROIs 24

3.4 Averaged neural RDMs for all subjects. Every dissimilarity matrix (24 x 24) is scaled into [0,1] and rank transformed independently. 26

3.5 Comparison of neural and model RDMs. Gray bands across the graphs show the noise ceiling, horizontal black lines show significant differences between models, and significant similarity to the ROI at the $p<0.05$ FDR corrected level is shown by the asterisk symbol (*). 27

3.6 Aracy minus chance results from the decoding analysis averaged over subjects. Successful decodings are marked with an asterisk "*" symbol. 28

List of Tables

3.1 Cluster number, peak threshold and peak coordinates of ROIs. . . 24

3.2 Comparison of neural RDMs and model RDMs. Kendall's Tau, Spearman's p and noise ceiling values are calculated. 27

3.3 Repeated ANOVA results of decoding values 29

Chapter 1

Introduction

1.1 Action Perception

Action perception is a fundamental function of the brain, enabling animals to identify and respond to threats and opportunities within their environment. Moreover, for humans, it is essential for social interactions, communication, and collaboration. Visual perception of action is a complex process that requires interpreting dynamic visual stimuli and predicting the movements and intentions of others.

Like other visual perception processes, it begins when the light from moving objects, captured by the eyes, falls on the photoreceptors of the retina and is converted into electrical signals. Then, these signals are relayed via the optic nerve to the first station of visual processing: the primary visual cortex (V1) [9]. Edges, basic movement, and changes in the light are processed in the primary visual cortex [10]. The signals are then conveyed to V2 and higher visual areas. These regions add color and more complex motion information to the current visual model [11]. Finally, the signals are sent to the parietal and temporal lobes for further processing. The visual system has two separate processing streams: one goes through the temporal lobe, called the ventral system, and one goes

through the parietal cortex, called the dorsal system.

The dorsal pathway specializes in perceiving the spatial aspects of the action, including the location, movement, and relationships of objects [12] and communicates with the premotor cortex for action planning [13]. Within the dorsal pathway, there are regions known to contain specialized cells sensitive to the direction of object motion, such as V5/MT+ [14]. In parallel to the dorsal pathway, visual information also progresses along the ventral pathway. Across this stream, areas in the temporal cortex process the object's identity. This pathway contains specialized cells, particularly in areas like the inferotemporal cortex and the fusiform face area, for perceiving object features, including shape, color, and texture [15].

Action perception is a complex process involving numerous brain regions, including early visual areas. However, specific regions are particularly crucial for understanding actions. A meta-analysis of action observation studies revealed consistent activation of a network of brain areas (Figure 1.1), now termed the Action Observation Network (AON) [1] [16] [17]. This network's core regions include the posterior superior temporal sulcus (pSTS), parietal, and premotor cortex. The locations of these regions can be seen in Figure 1.2.

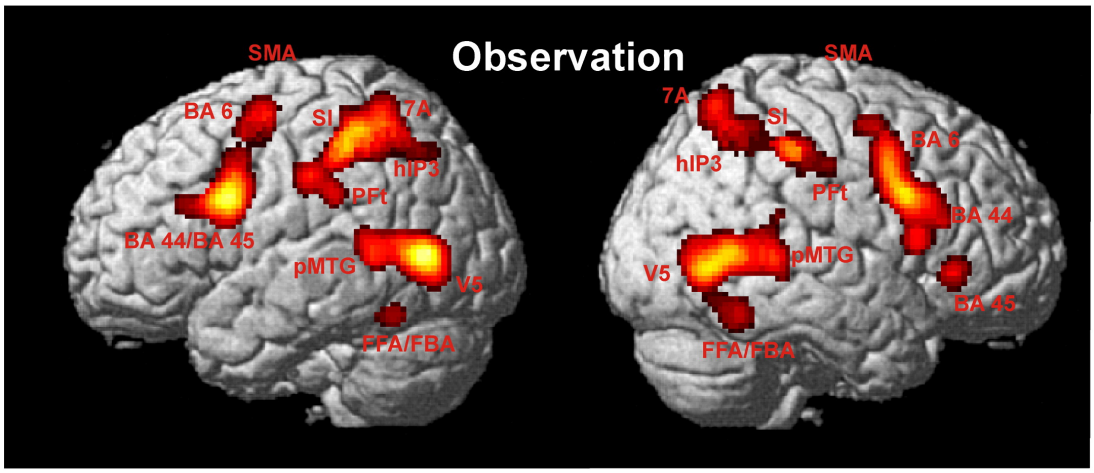

Figure 1.1: Meta-analysis results for action observation [1]. pMTG posterior middle temporal gyrus, SMA supplementary motor area; BA 44, 45: Broca's area [2]; BA 6: lateral premotor cortex [3]; SI: primary somatosensory cortex (BA 2 [4]); 7A: superior parietal area [5]; PFt: inferior parietal area [6] [7]; hIP3: intraparietal area [5]; V5: extrastriate visual area [8]. (Reprinted with permission.)

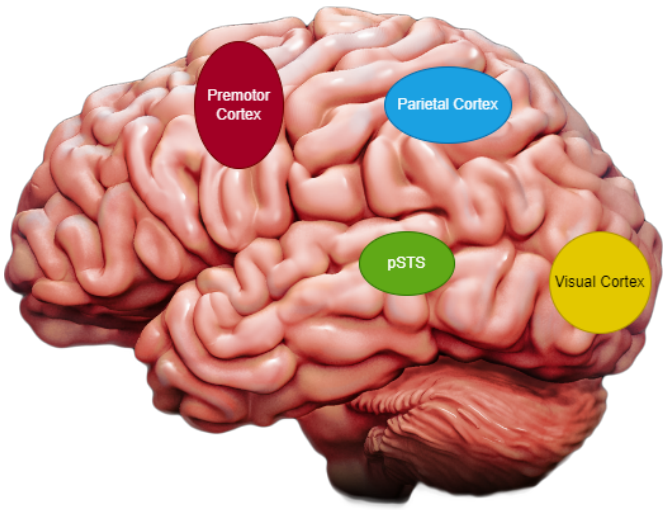

Figure 1.2: The core brain regions of AON. pSTS: posterior superior temporal sulcus

1.2 Role of Attention in Perception

Neuroimaging studies on the AON often involve evaluating brain activity while participants passive action observation without performing any specific task. However, this approach may not fully capture the complexity of real-world action perception, where we typically observe actions with specific intentions or mental states. In modern neuroscience, visual perception is believed to include both the bottom-up and top-down processes [18]. The limitations of passive observation studies highlight the need to consider the dynamic interplay between bottom-up sensory information and top-down cognitive factors, essential for a holistic understanding of how visual perception operates in real-world contexts.

While many action observation models have focused solely on bottom-up processing [19], recent research by Kilner et al. [20] and Urgen & Saygin [21] underscores the importance of taking into account top-down processes as well, such as expectation and prediction. Attention, also a top-down process, is known to play a significant role in shaping perception. In real-world scenarios, we do not view the action passively; we actively direct our attention to specific elements of observed actions. Neglecting top-down attentional processes in action perception studies hinders our understanding of how top-down modulation shapes action perception.

Attention is a cognitive process that allows the brain to focus on specific and desired information while ignoring or minimizing distracting elements. This process coordinates the allocation of cognitive resources, ensuring the efficient processing of sensory data. It can be directed either voluntarily, such as when we consciously focus on a task (top-down), or involuntarily, such as when a sudden loud noise captures our attention (bottom-up) [22]. It plays a significant role in various cognitive processes like perception, learning, memory, and problem-solving, and is crucial for effective information processing.

Attention also plays a critical role in shaping visual perception, as indicated by significant research in neuroscience. These studies demonstrate that attention

can shape the activities of different neural populations in a top-down manner [23]. Attention alters the firing rates of sensory neurons, often leading to a stronger response to the attended stimulus [24], thereby potentially enhancing processing and improving performance in tasks that utilize visual stimuli [25].

Many studies have revealed that some attention processes operate at the object level while others operate based on features such as color, shape, and motion. When attention is directed toward features, it is termed feature-based attention [26]. In the visual cortex, there is an observed increase in the activity of neuron groups that prefer the attended feature, coupled with a decrease in the activity of neuron groups that prefer the unattended features [27], similar to other attention processes. These findings suggest that feature-based attention are complex brain process that significantly influence visual perception.

1.3 Previous Research

A limited number of studies have focused on how attentional mechanisms may influence the brain regions within the AON. For example, in one study by Stehr et al., [28], top-down influences on action observation were investigated using multivariate pattern analysis. In the experiments, participants attended to different features of action -the kinematics, the goal, or the identity of the virtual actor- while watching the same set of stimuli. The authors investigated the effects on the pSTS and inferior frontal cortex (IFC). They observed that the activity in these brain regions varied according to attention instructions. They found that when participants attended action kinematics, the activity was most prominent, thus easily decodable in the right pSTS. Also, attending to action goals increased the decoding performance in the right IFC. This study demonstrated that the AON is dynamic and modulated by top-down effects.

In the study conducted by Orban et al. [29], the authors focused on the distinct roles of the layers of the AON (occipitotemporal, parietal, and premotor). They investigated whether the information at the parietal level is sufficient for

action discrimination via the two-alternative forced-choice task or whether the information from the other two levels is also required. They used a task-based attention modulation paradigm for their fMRI experiments, in which participants needed to discriminate between two actions, two actors, or two object colors. They found that relative to color and actor, action discrimination activated the putative human anterior intraparietal sulcus (phAIP) area in the parietal cortex. Thus, they showed that the parietal region plays a major role in determining the action identity. Additionally, the results indicate that even when stimuli have the same visual features, merely changing the task can result in different activation patterns in the AON.

In another study conducted by Shahdloo et al., [30], the authors focused on the effect of attention on action perception. In the fMRI experiment, participants viewed a large set of varied stimuli derived from natural movies. They performed a visual search task, looking for locomotion or communication actions. The authors observed that attending to the action category led to tuning shifts towards the target in semantic representations throughout the neocortex, with the change depending on the intrinsic selectivity pattern of the cortex. These results suggest that attention mechanisms in the brain enhance task performance by shifting the selectivity for action classes, demonstrating the task-dependent dynamic nature of the brain.

1.4 Current Study

Three core features are essential: the actor initiating the action, the effector specifying the body parts involved, and the target, which can be an object, another person, or even the environment. These core elements are further intertwined with higher-level concepts like context, agency, and decision-making. While some studies explored the actor and action classes within various tasks, the focus often narrowed solely to manipulation actions (grasping, pushing). These studies do not systematically investigate attentional modulation across the entire AON when attention is directed to the action's core features. This lack of focus on

action features and attention represents a significant gap in our understanding of how we perceive actions.

This study examines the influence of feature-based attention on brain regions related to action perception. The pSTS, parietal, and premotor regions within the AON were selected for this investigation. A multi-level analysis revealed the interactions between top-down mechanisms and action perception. First, regions of interest (ROIs) were localized through a passive viewing fMRI session. Univariate analysis, representational similarity analysis, and decoding analysis were then applied to uncover details about the interplay between task-based attention and action observation. Specifically, we investigated whether attending to different features of an action (actor, effector, and target) uniquely affects different layers of the AON (pSTS, parietal, and premotor). This research helps to reveal dynamic neural activity patterns of action perception modulated by top-down attention processes.

Chapter 2

Methods

2.1 Participants

A total of 30 healthy individuals, aged between 21 and 31, with normal or corrected vision, took part in a two-session fMRI experiment. After excluding 3 participants due to technical issues, the final sample consisted of 27 individuals (12 females). The Human Research Ethics Committee of Bilkent University approved the study and all participants gave their written consent before the experiment.

2.2 Stimuli and Experimental Design

2.2.1 Stimuli

Eight action videos were recorded in the G building Psychology lab at Bilkent University to show to participants during the fMRI experiments. All videos depicted the action of "pushing" but with variations in the actor (female or male), the effector (hand or foot), and the target (object or human). Figure 2.1

displays a frame from each video.

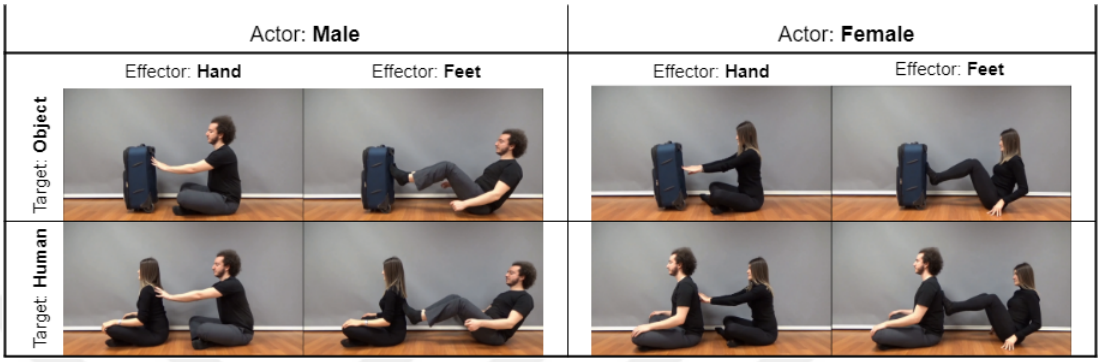

Figure 2.1: The stimuli for fMRI experiments: One frame from each video, demonstrating the action with variations in actor, effector, and target.

The Sony HDR-CX405 Handycam Video Camera was used to record the videos at 50 fps and 1280x720 resolution. While shooting the videos, specific criteria were met. The actors were in the same position at the beginning and end of the videos, posed in a cross-legged position with hands on their knees. The distance between the actors and the camera was consistent in all videos, and the action was positioned symmetrically in the video frame. The actors practiced for smooth transitions, consistent force, and movement velocity, avoiding expressing any emotions before recording. The actors' clothing was chosen to avoid capturing attention and to be similar to each other (black top, black pants).

2.2.2 Experimental Design and Setup

There are two fMRI sessions in this study. In the first session, participants watched the videos and performed different tasks related to them. In the second session, participants viewed the same stimuli without performing any task.

The first session consists of 8 runs, each lasting approximately 8 minutes. The tasks in the active session include 3 different attention conditions, which are defined as Actor, Effector, and Target blocks. Before each block, participants were instructed to perform the corresponding task (Figure 2.2, top section). Within each run, each block is presented two times. The 3 attention blocks are grouped

to form a set, and within each set, the attention blocks are randomized. There were 12-second rest blocks at the beginning of the experiment, between the sets, and at the end of the experiment.

In each block, participants were shown the videos in random order (as illustrated in Figure 2.2, bottom section). After each video, they had 2.5 seconds to respond to the question. Then, interstimulus intervals between 3 and 4 seconds were inserted, during which they fixated on the screen. The average length of these intervals was 3.5 seconds.

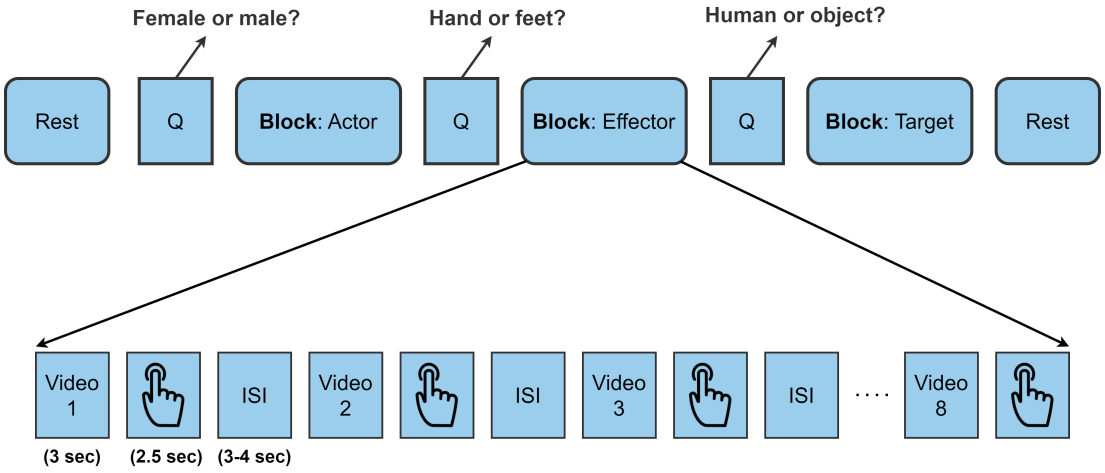

Figure 2.2: Experimental design for a set (top) and a block (bottom). The hand figure represents the response interval. ISI: interstimulus interval.

A practice session was held to familiarize participants with the experiment and stimuli. During this brief trial, each block was shown once, featuring two preselected videos representing the full range of variations ("female, hand, object" and "male, feet, human").

In the second session, participants watched the same set of videos without performing any task. This passive session consisted of 4 runs, each lasting approximately 6 minutes. In each run, participants viewed 6 blocks of videos, resulting in each video being presented 24 times (6 blocks x 4 runs). The data from this session is used to extract ROIs and univariate analysis.

Participants viewed the video stimuli in the MRI machine on a TELEMED screen (refresh rate: 60 Hz, resolution: 1920x1080) reflected in a head coil mirror. Videos were displayed at 550x340 pixels on a gray background. PsychoPy and custom Python functions were utilized for stimulus presentation and response collection.

2.2.3 Data Acquisition

Brain activity was recorded using a 32-channel head coil on a 3T Siemens TimTrio MRI scanner at Bilkent University's National Magnetic Resonance Research Center (UMRAM). Soft cushions minimized head movement, while earplugs protected participants from the MRI machine's noise.

Prior to the functional scans, high-resolution T1-weighted structural scans of participants' brains were acquired for both experiments (TR=2600 ms, TE=2.92 ms, flip angle=12°, FoV read=256 mm, phase FoV=%87.5, 176 slices, and $1\times1\times1$ mm^3 resolution). Then, for the active session, 168 functional scans and for the passive session 129 functional scans were obtained using gradient echo-planar imaging (TR=3000 ms, TE=22 ms, flip angle=90°, 64 x 64 matrix, FoV read=192 mm, 43 slices with a thickness of 2.5 mm and a resolution of $3\times3\times2.5$ mm^3).

2.2.3.1 Preprocessing with fMRIPrep

Results included in this manuscript came from preprocessing performed using fMRIPrep 21.0.1 [31], a Nipype [32] based tool. Each T1w (T1-weighted) volume was corrected for INU (intensity non-uniformity) using N4BiasFieldCorrection v2.1.0 [33] and skull-stripped using antsBrainExtraction.sh v2.1.0 (using the OASIS template). Brain surfaces were reconstructed using recon-all from FreeSurfer v6.0.0 [34], and the brain mask estimated previously was refined with a custom variation of the method to reconcile ANTs-derived and FreeSurfer-derived segmentations of the cortical gray-matter of Mindboggle [35]. Spatial normalization

to the ICBM 152 Nonlinear Asymmetrical template version 2009c [36] was performed through nonlinear registration with the antsRegistration tool of ANTs v2.1.0 [37], using brain-extracted versions of both T1w volume and template. Brain tissue segmentation of cerebrospinal fluid (CSF), white-matter (WM) and gray-matter (GM) was performed on the brain-extracted T1w using fast [38] (FSL v5.0.9).

Functional data was slice time corrected using 3dTshift from AFNI v16.2.07 [39] and motion corrected using mcflirt (FSL v5.0.9 [40]). This was followed by co-registration to the corresponding T1w using boundary-based registration [41] with 9 degrees of freedom, using bbregister (FreeSurfer v6.0.0). Motion correcting transformations, BOLD-to-T1w transformation and T1w-to-template (MNI) warp were concatenated and applied in a single step using antsApplyTransforms (ANTs v2.1.0) using Lanczos interpolation.

Physiological noise regressors were extracted applying CompCor [42]. Principal components were estimated for the two CompCor variants: temporal (tCompCor) and anatomical (aCompCor). A mask to exclude signal with cortical origin was obtained by eroding the brain mask, ensuring it only contained subcortical structures. Six tCompCor components were then calculated including only the top 5% variable voxels within that subcortical mask. For aCompCor, six components were calculated within the intersection of the subcortical mask and the union of CSF and WM masks calculated in T1w space, after their projection to the native space of each functional run. Frame-wise displacement [43] as calculated for each functional run using the implementation of Nipype.

Many internal operations of fMRIPrep use Nilearn [44], principally within the BOLD-processing workflow. For more details of the pipeline see http://fmriprep.readthedocs.io/en/latest/workflows.html.

2.3 Behavioral Analysis

The reaction times and accuracy values from the active session were examined. To see whether the tasks varied in difficulty, we performed one-way repeated measures ANOVA to compare the three tasks.

2.4 Univariate Analysis

Following preprocessing, we conducted univariate analysis using SPM12 software. We employed the general linear model (GLM) to analyze both the active and passive session data.

In the passive session analysis, the GLM included these regressors: instruction, videos, rest, ISI, and 6 head movements regressors (3 for rotations, 3 for translations). Functional scans were smoothed with a full width at half maximum (FWHM) = 4mm kernel, which was used for univariate analysis and visualization purposes. We then compared brain activity during action videos to rest, identifying specific ROIs within the AON for further analysis. These ROIs included pSTS, parietal, and premotor regions in both hemispheres.

In the active session, we applied different modeling steps for each type of further analysis. For univariate analysis, the GLM included one regressor for each task (actor, effector, and target) and one for instruction, rest, and ISI. Additionally, it included 6 head motion parameters. For Representational Similarity Analysis, each video viewed under a different task was treated as a separate regressor (3 tasks x 8 videos = 24 video regressors). The rest of the regressors were as before. For Decoding Analysis, each trial was defined as unique variables (2 trials x 3 tasks x 8 videos = 48 video regressors), keeping other regressors the same.

Contrast analyses were performed to highlight differences between attention conditions for further univariate analysis. For the active session, it involved

comparing each attention task to the rest condition and also contrasting all tasks combined with rest. The beta images were smoothed to enhance visualization of the active brain regions.

2.5 Representational Similarity Analysis

Representational Similarity Analysis (RSA) is a computational technique used in cognitive neuroscience to compare patterns of neural activity elicited by different stimuli [45] [46]. By generating a Representational Dissimilarity Matrix (RDM), RSA quantifies the differences between neural responses, allowing researchers to explore how information is represented across different brain areas. A standard measure for calculating these dissimilarities is correlation or Euclidean distance. By comparing RDMs across brain regions or between subjects, we discover how similar the information is represented in the brain. Also, RDMs can be compared with theoretical models, which help scientists to test different hypotheses about cognitive processes. This approach is called model-based RSA, which was applied in this study. Because of its adaptability, RSA allows for cross-modal comparisons between behavioral measurements, computational models, and neural data, offering a comprehensive framework for studying the neurological underpinnings of cognition.

We applied model-based RSA to reveal which models reflect the neural activity in the selected ROIs. Rsatoolbox [47] was used to implement the analysis. In the univariate analysis, modeled video regressors (3 tasks x 8 videos) were contrasted with the rest. The resulting spmT files were used as inputs for RSA.

Six distinct models were generated to compare with the neural Representational Dissimilarity Matrices (RDMs). In Figure 2.3, you can see the structure of each dissimilarity matrix. Each matrix is 24 x 24 since the videos that are watched under different tasks are defined as distinct variables (3 tasks x 8 videos).

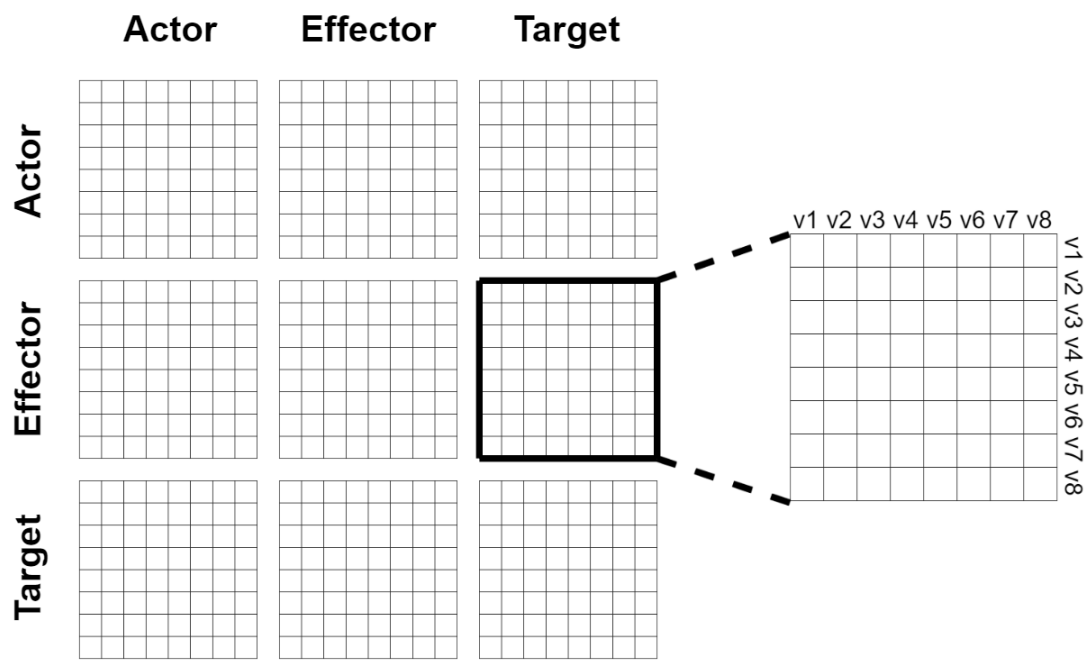

Figure 2.3: The structure of the model RDMs. Its size is 24x24, representing 8 action videos under 3 different attention tasks

The initial three model RDMs are represented as binary matrices, depicting the actor, effector, and target features of the videos. A value of 1 means dissimilarity, while 0 indicates similarity within each attribute. For instance, in the Actor model, same-gender pairs were coded as 0 and mixed-gender pairs as 1. The fourth model, the task model, also utilized a binary matrix to differentiate between identical and different task values. Identical tasks were assigned 0, and different tasks 1. The fifth model, the visual model, assessed video similarities using Matlab's structural similarity function, which considers luminance, contrast, and structure. The output values ranged from 0 (perfect similarity) to 1 (complete dissimilarity). Finally, a random model was included as a control. Figure 2.4 illustrates the structure of these models and their visual representation.

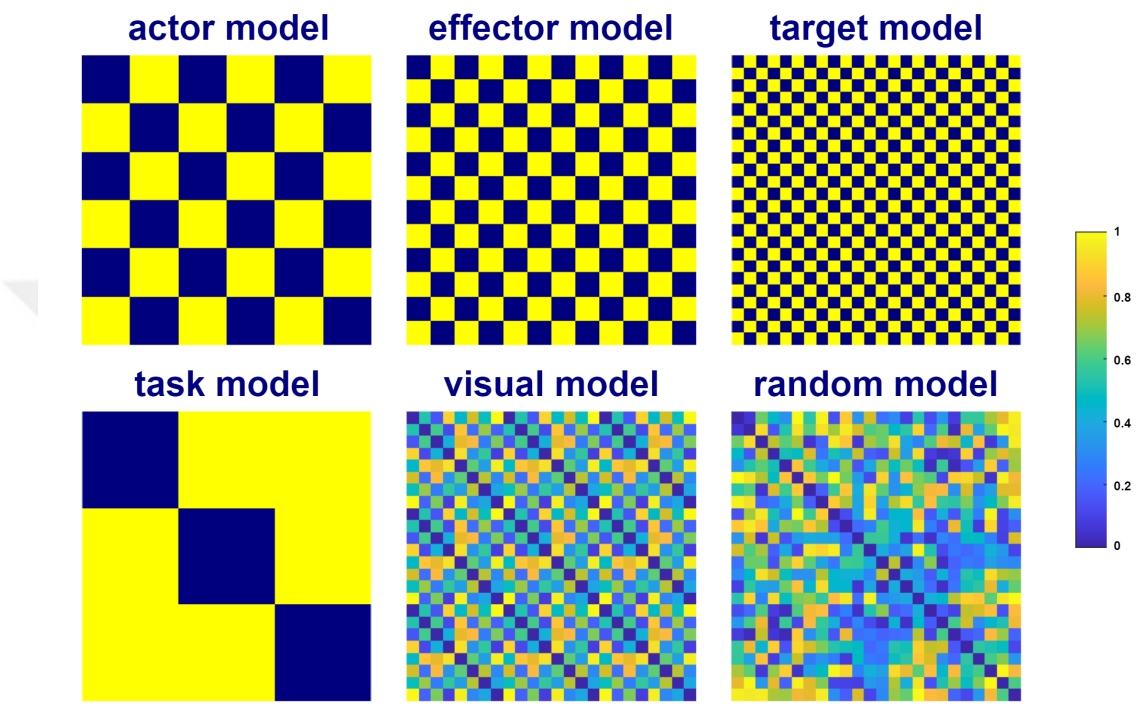

Figure 2.4: 6 model RDMs, to be compared with neural RDMs for each region of interest (ROI). These models represent different aspects: actor, effector, and target models capture video features; the task model represents unique tasks; the visual model reflects visual similarity between videos; and the random model, generated with random numbers, acts as a control model for comparison.

2.6 Decoding Analysis

Decoding analysis is a computational technique that uses machine learning methods to infer information in a brain region based on how well specific stimuli can be classified. Main idea of this analysis is to train machine learning models on some part of the neural data and then try to decode or classify the desired variables on remaining neural data. Support vector machines (SVM), logistic regression or neural networks can be used for this method. Decoding analysis contributes our understanding of the neural coding mechanisms by revealing how different

patterns of neural activity correlate to particular stimuli [48] [49].

To investigate neural activity within the ROIs, we employed Decoding Analysis using the decoding toolbox [50]. Our main goal was to see if we could discriminate different features (like actor, effector, and target) within these regions under different attentional tasks.

We conducted 54 individual analyses to examine how well the ROIs distinguished between two different features. We used brain activity patterns from different hemispheres (left/right), specific brain areas (pSTS, parietal, premotor), and different tasks (actor, effector, target). We applied a machine learning technique (linear SVM) [51] to these brain patterns to see how accurately it could predict the features in the videos.

To ensure reliable results, we used a "leave-one-run-out" cross-validation method, which means we trained the machine learning model on all but one run and tested its performance on the remaining data point. This process was repeated, leaving out a different run each time.

We then calculated how often the machine learning model made correct predictions (decoding accuracy). To determine if the predictions were better than chance (50%), we used a t-test. Additionally, we used a repeated-measures ANOVA test to explore how different factors (hemisphere, ROI, task, and features) influenced the model's performance. This method allowed us to understand if there were any significant differences or interactions between these factors.

Chapter 3

Results

3.1 Behavioral Results

Behavioral analysis was performed on responses to control if the participants could perform the task and to check if there was a difference in task difficulties. The average accuracy rate for all tasks was 95.5% (sd=+-7.9%) across participants. The accuracy was 95.3% (sd =+- 7.6%) for the actor task, 95.9% (sd =+-8.3%) for the effector task, and 95.5% (sd =+-8.1%) for the target task. A one-way ANOVA was run to compare the task accuracy rates. According to the findings, there are no statistically significant differences between these tasks ($F(2, 78) = 0.04$, $p = 0.964$).

In the response time analysis, the inaccurate responses were not included. The average response time across all tasks was 0.80 seconds (sd=+-0.18 seconds). The average response time was 0.81s (sd = -+ 0.20) for the actor task, 0.78s (sd = +-0.18) for the effector task, and 0.81s (sd = +-0.17) for the target task. A one-way ANOVA was run to compare the task response times. There are no statistically significant differences between these tasks regarding response time ($F(2, 78) = 0.21$, $p = 0.812$).

3.2 Univariate Analysis Results and ROI Selection

3.2.1 Data Cleaning

Of the 30 total participants, one was excluded from the analysis due to technical problems during scanning. For the remaining 29 participants, motion profiles were examined using motion regressors extracted from preprocessing outcomes. Runs with a total movement of one voxel size or half-voxel size spikes were excluded from further analysis. This resulted in the complete exclusion of two participants due to the removal of more than half of their runs, leaving a total of 27 participants. Additionally, in the active session, two runs from two participants and one run from three participants were removed. In the passive session, one run from one participant was excluded.

3.2.2 Univariate Results

For the passive session, to see whether the videos activated the AON when participants watched them, we checked the "videos minus rest" contrast. As can be seen from Figure 5 (top section), we observed activation in early visual areas such as V1, V2, and V3, in occipitotemporal cortex such as MT cluster and posterior superior temporal sulcus, and in the posterior parietal cortex such as PGp region at FWE corrected $p<0.05$ significance threshold level. At uncorrected $p<0.001$ threshold level, we observed more regions in the AON. For example, phAIP, PGp, PGa, PFt, PFpop, PFm, PFcm, PF [6] in the posterior parietal cortex and in the premotor cortex. This activation map obtained from $p<0.001$ uncorrected level is used as activation borders in both Figure 3.1 and Figure 3.2.

For the active session, we also check the activation obtained from all movies (regardless of task) contrasted with rest at FWE corrected $p<0.05$ significance

level. The resulting activation maps showed similar activation patterns to passive sessions, with extended activation in the posterior parietal cortex, premotor cortex, and some frontal areas. DIPSA, DIPSM, phAIP (extended) [52], BA2 (extended), BA3, BA4, and PMm are some of the regions that have activation in active session (Figure 3.1, bottom).

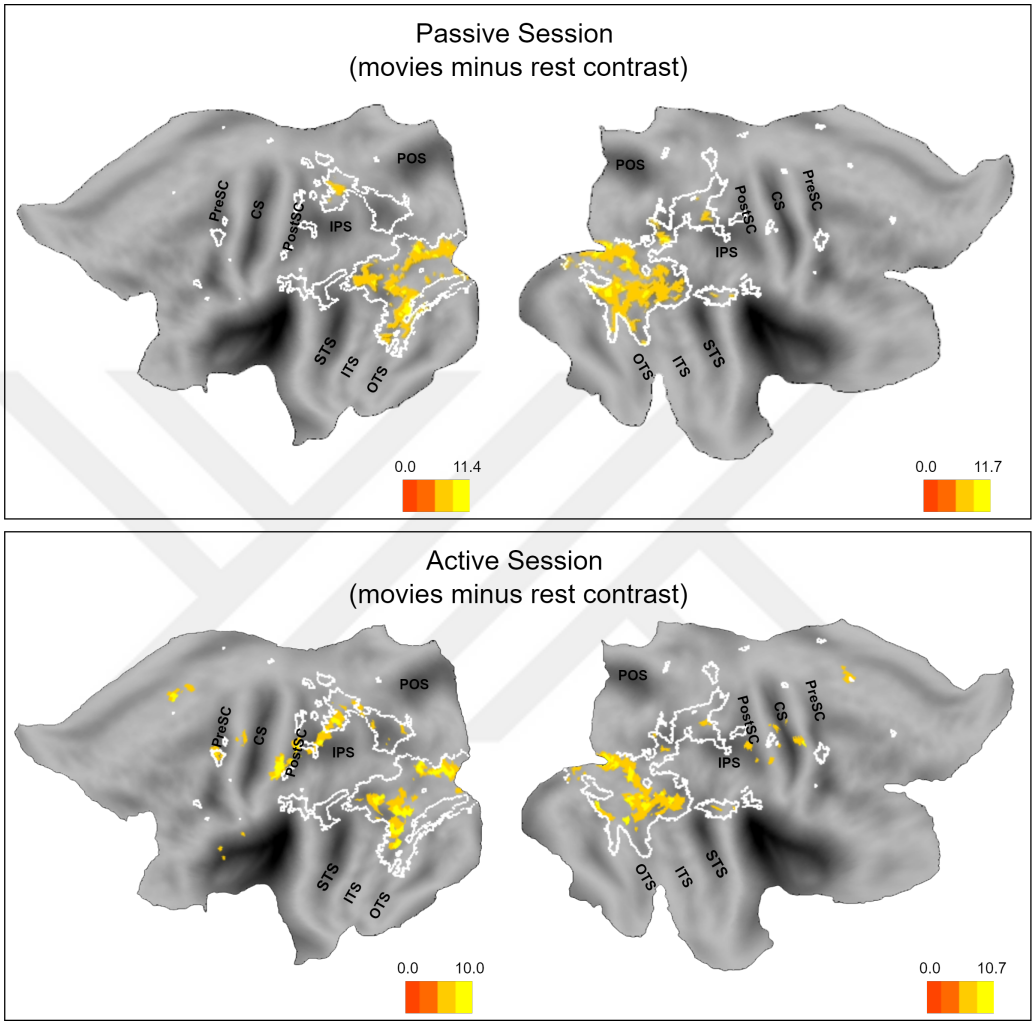

Figure 3.1: Activation maps resulted from videos minus rest contrast (FWE corrected, $p<0.05$) of passive session (top) and active session (bottom). The white borders show the activation area of the passive session at $p<0.001$ uncorrected level. The visualization was done with Caret5 software. Landmarks are indicated in black: PreSC (Pre-central sulcus), CS (Central sulcus), PostCS (Post-central sulcus), IPS (intra-parietal sulcus), POS (parieto-occipital sulcus), STS (superior temporal sulcus), ITS (inferior temporal sulcus), OTS (occipito-temporal sulcus).

Next, we visualized the activation maps of each task. The resulting activation maps are very similar to all tasks with rest contrast and can be seen in Figure 3.2.

The univariate map of each task is similar, with slight task and hemisphere-dependent differences. For example, the DIPSA region was active across all tasks in the left hemisphere but only during the actor task in the right hemisphere. DIPSM was active in effector and target tasks within the left hemisphere, while in the right hemisphere, DIPSM showed activation at its DIPSA border again in effector and target tasks, not in the actor task. The OP1 region was active only for the effector task in the right hemisphere. The premotor activation area derived from [53] was active across all tasks in the left hemisphere but inactive in the right hemisphere.

Additionally, premotor dorsal, medial, and ventral regions were all active within the left hemisphere. In contrast, in the right hemisphere, only the premotor medial region showed activation, which was limited to the actor and target tasks. Finally, the lateral occipitotemporal cortex is consistently activated across all tasks and both hemispheres, specifically in the middle temporal gyrus (MTG), MT+, and occipitotemporal sulcus (OTS).

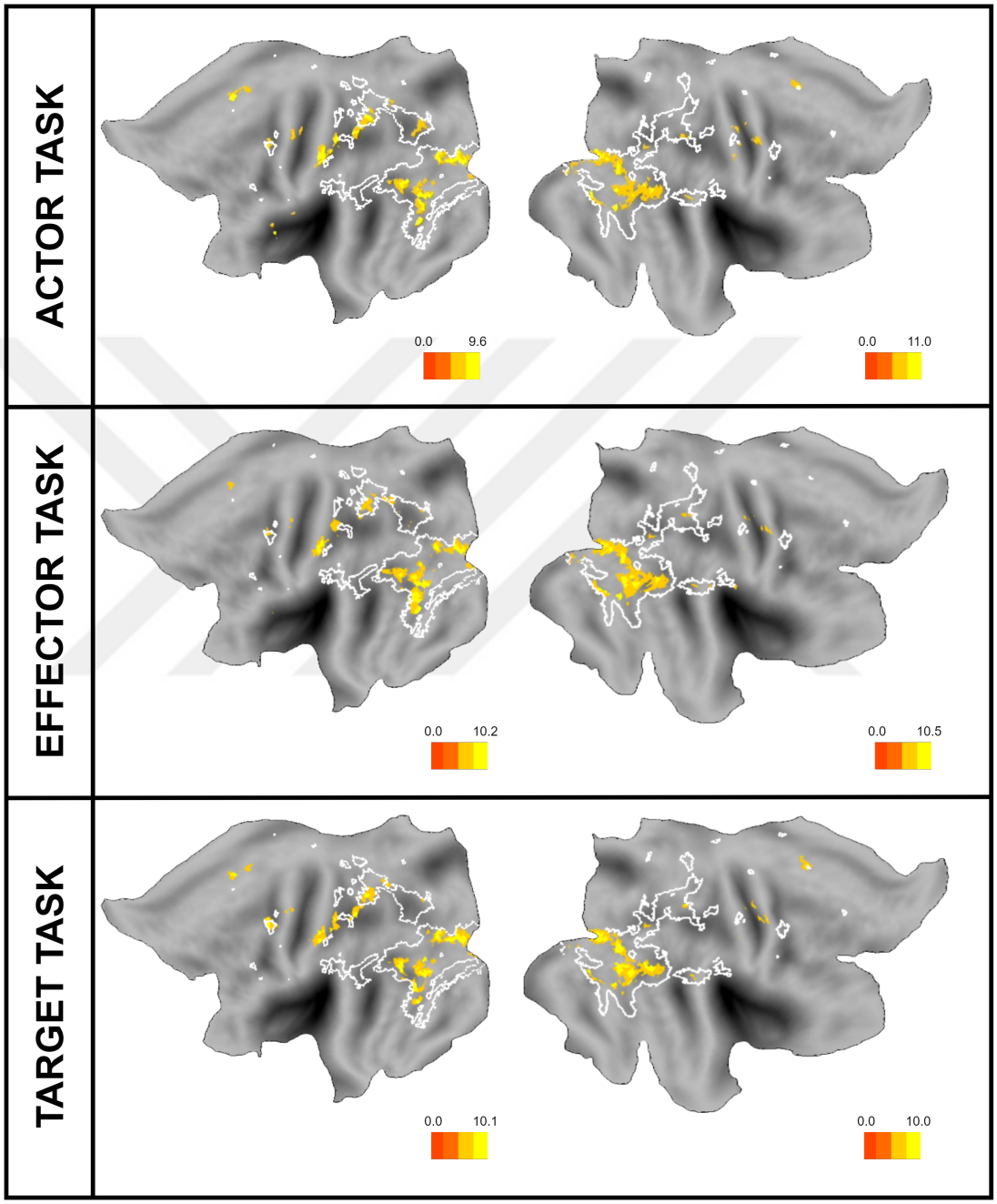

Figure 3.2: Activation maps of actor task (top), effector task (middle) and target task (bottom). All activation maps were derived from videos and rest contrast for significance level at $p<0.05$ with FWE correction. The white borders are representation of passive session videos and rest condition at significance level at $p<0.001$, uncorrected.

3.2.3 Identification of ROIs

We used passive session data to extract the regions of interest (ROIs) for further analysis. We used the "movies minus rest" contrast at a threshold of $p<0.001$ uncorrected to be able to include all levels of the AON (pSTS, parietal, and premotor). First, we used AAL atlas [54] to identify the brain regions that include our ROIs (Temporal_Sup for pSTS, the union of Parietal_Inf and Parietal_Sup for the parietal cortex, and Precentral for the premotor cortex). Then, we used these AAL brain regions to mask the group-level analysis. The activated voxel group inside the corresponding mask was used as the ROI. The ROIs were visualized using MRIcroGL (Figure 3.2), and the coordinates of ROIs can be found in Table 1.

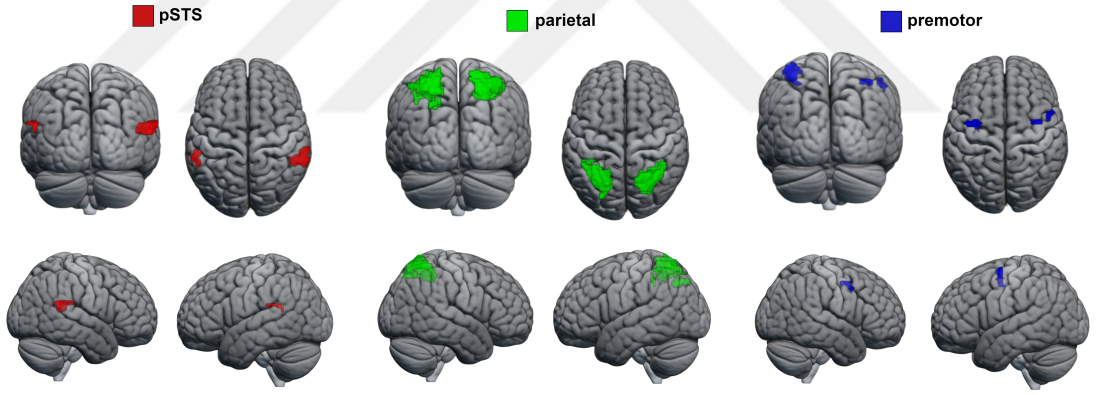

Figure 3.3: Visualization of ROIs

Table 3.1: Cluster number, peak threshold and peak coordinates of ROIs.

Region of Interest	**Left Hemisphere**			**Right Hemisphere**		
	Cluster Number	Peak Threshold	Peak Coordinates	Cluster Number	Peak Threshold	Peak Coordinates
pSTS	k=27	t=4.98	-54 -46 19	k=114	t=6.47	54 -42 19
parietal	k=440	t=9.11	-28 -58 59	k=459	t=8.19	36 -54 56
premotor	k=68	t=5.95	-36 -4 52	k=17 k=22	t=5.14 t=4.92	38 -4 49 50 2 46

3.3 Representational Similarity Analysis Results

For each ROI, neural RDMs were created using the correlation distance between the spmT values of each variable (Figure 3.3). As a next step, neural RDMs were compared with model RDMs using Kendall's Tau values, and a one-sided Wilcoxon signed-rank random-effects test corrected for multiple comparisons (FDR) at a threshold of $p<0.05$ was conducted. Also, noise ceiling upper and lower bounds were calculated using Kendall's Tau values by estimating a hypothetical model with the highest possible average correlation to the reference RDM. Model RDM and neural RDM comparison values can be found in Figure 3.4.

Only the task model showed a significant correlation ($p<0.05$, FDR adjusted) with all neural RDMs for all ROIs; no other model showed any significant correlation. Additionally, the task model's Kendall's Tau value (0.2413) in the right premotor reached the noise ceiling (0.2266, 0.3068). Table 2 contains Kendall's Tau and noise ceiling values for each ROI and model.

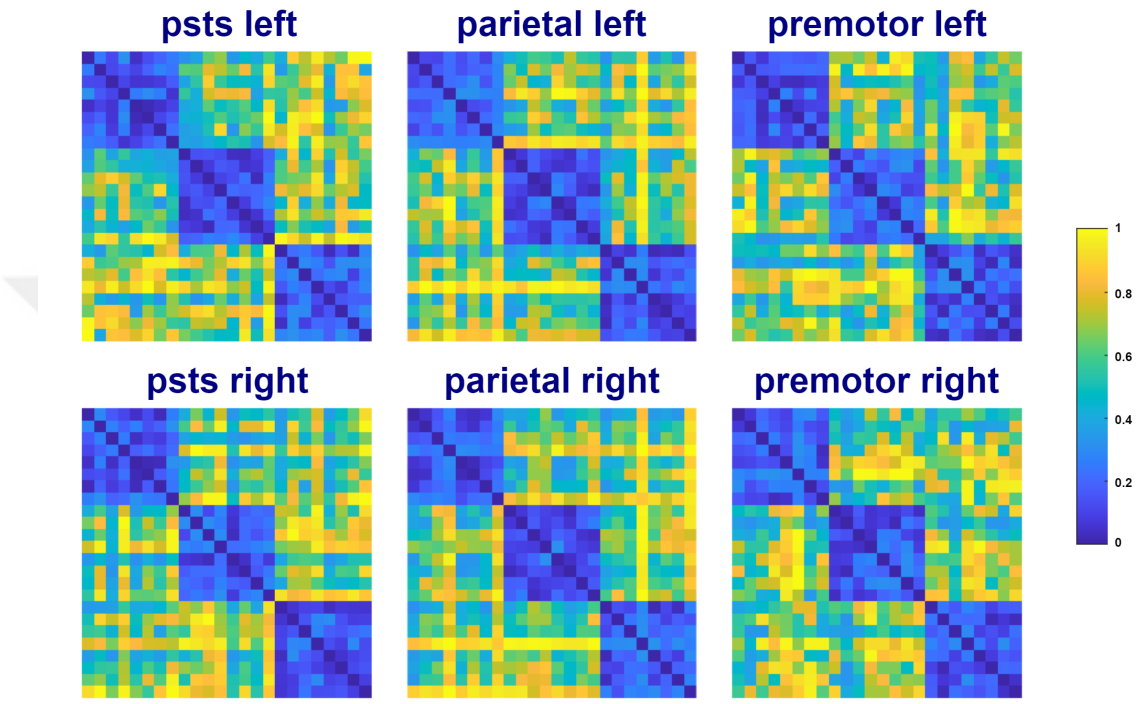

Figure 3.4: Averaged neural RDMs for all subjects. Every dissimilarity matrix (24 x 24) is scaled into [0,1] and rank transformed independently.

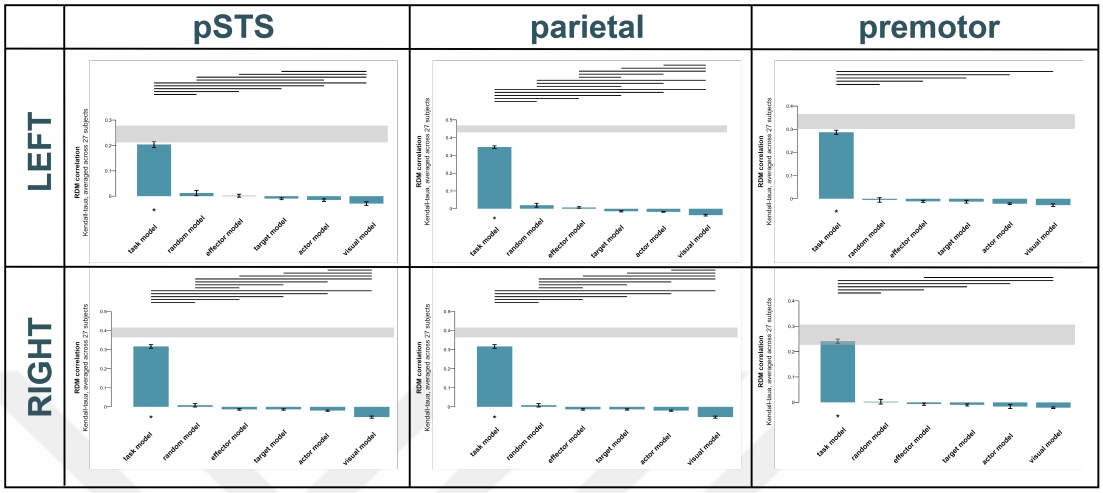

Figure 3.5: Comparison of neural and model RDMs. Gray bands across the graphs show the noise ceiling, horizontal black lines show significant differences between models, and significant similarity to the ROI at the $p<0.05$ FDR corrected level is shown by the asterisk symbol (*).

Table 3.2: Comparison of neural RDMs and model RDMs. Kendall's Tau, Spearman's p and noise ceiling values are calculated.

	ROI	pSTS left	pSTS right	parietal left	parietal right	premotor left	premotor right
Actor	**Kendall's Tau**	-0.0152	-0.0199	-0.0174	-0.0180	-0.0216	-0.0211
Model	**p-value**	1.00	1.00	1.00	1.00	1.00	1.00
Effector	**Kendall's Tau**	0.0020	-0.0133	0.0074	0.0031	-0.0113	-0.0068
Model	**p-value**	0.43	1.00	0.13	0.66	1.00	0.92
Target	**Kendall's Tau**	-0.0098	-0.0135	-0.0138	-0.0063	-0.0124	-0.0101
Model	**p-value**	0.99	1.00	1.00	0.99	0.99	0.99
Task	**Kendall's Tau**	**0.2038**	**0.3171**	**0.3470**	**0.3122**	**0.2870**	**0.2413**
Model	**p-value**	**0.00**	**0.00**	**0.00**	**0.00**	**0.00**	**0.00**
Visual	**Kendall's Tau**	-0.0291	-0.0537	-0.0362	-0.0321	-0.0277	-0.0165
Model	**p-value**	1.00	1.00	1.00	1.00	1.00	0.98
Random	**Kendall's Tau**	0.0126	0.0084	0.0200	0.0094	-0.0049	0.0025
Model	**p-value**	0.08	0.11	0.06	0.13	0.69	0.42
	Noise Ceiling	(0.2118, 0.2784)	(0.3642, 0.4157)	(0.4289, 0.4691)	(0.3816, 0.4261)	(0.3015, 0.3654)	**(0.2266, 0.3068)**

3.4 Decoding Analysis Results

The features of the videos, which are "female vs. male", "hand vs. feet", and "human vs. object" was decoded (binary classification) under separate tasks

(actor, effector, target) in each ROI (left/right pSTS, left/right parietal, left/right premotor). 54 decoding analyses were run (2 hemispheres X 3 ROIs X 3 tasks X 3 features). Linear support vector machines were trained separately for each decoding analysis. A one-sided t-test with decoding outcomes was conducted against the chance level (50%) to determine if the decodings were successful. Figure 3.5 shows the success of the decoding and accuracy minus chance levels for each decoding.

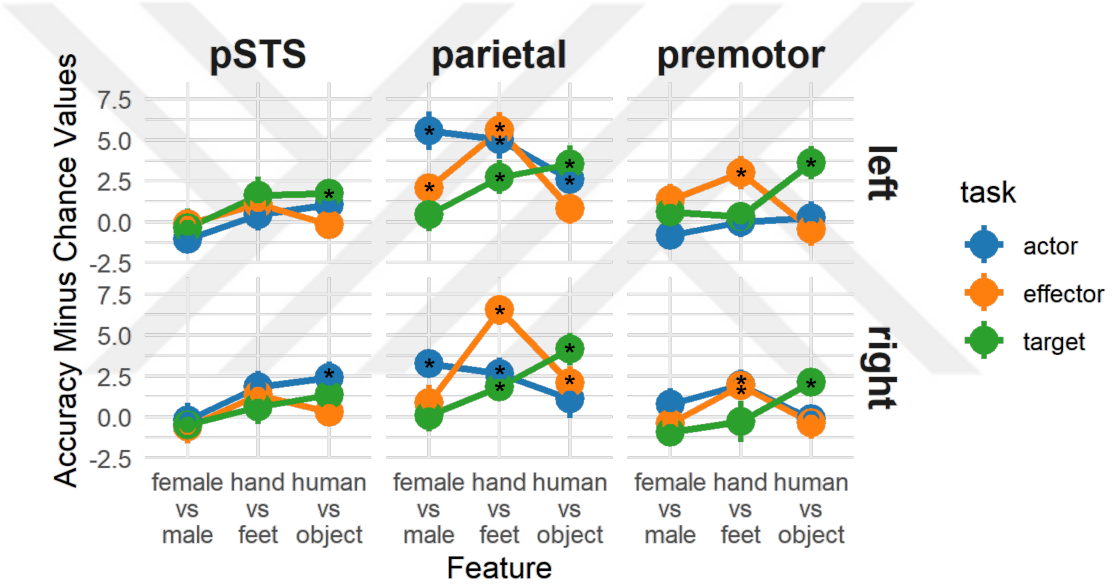

Figure 3.6: Aracy minus chance results from the decoding analysis averaged over subjects. Successful decodings are marked with an asterisk "*" symbol.

For the pSTS region, the decoding was successful for only the human vs. object feature, under the target task for the left hemisphere and under the actor task for the right hemisphere. All features could be decoded for the parietal cortex with slight task and hemisphere differences. Female vs. male classification was successful under the actor and effector tasks for the left hemisphere and only the actor task for the right hemisphere. Hand vs. feet classification was successful under all tasks and for both hemispheres. Human vs. object classification was successful under the actor and target tasks for the left hemisphere and under the effector and target tasks for the right hemisphere. For the premotor cortex, the female vs. male classification was unsuccessful under any task and hemisphere.

On the other hand, hand vs. feet classification was successful only under the effector task for the left hemisphere and under the actor and effector tasks for the right hemisphere. Also, human vs. object classification was successful under only the target task for both hemispheres.

To statistically investigate the decoding differences between the conditions, we used repeated measures ANOVA with the following variables included: 2 (Hemisphere) x 3 (ROI) x 3 (Task) x 3 (Feature). Table 3.3 provides an overview of the main impact and interaction statistics.

Table 3.3: Repeated ANOVA results of decoding values

2 (Hemisphere) x 3 (ROI) x 3 (Task) x 3 (Features) Repeated Measures ANOVA Results			
Cases	**F value**	**p value**	**eta squared**
hemi	1.433	0.242	-
roi	**48.236**	**<0.001**	**0.038**
task	0.130	0.879	-
feature	**7.003**	**0.002**	**0.015**
hemi * roi	0.905	0.411	-
hemi * task	0.526	0.594	-
roi * task	1.728	0.149	-
hemi * feature	0.581	0.563	-
roi * feature	1.535	0.197	-
task * feature	**6.702**	**<0.001**	**0.024**
hemi * roi * task	**3.443**	**0.011**	**0.007**
hemi * roi * feature	0.332	0.856	-
hemi * task * feature	0.485	0.747	-
roi * task * feature	**2.325**	**0.021**	**0.012**
hemi * roi * task * feature	0.324	0.956	-

From ANOVA results, it can be seen that there was a main effect of feature (F=7.003, p=0.002, eta squared=0.015) and ROI (F=48.236, p<0.001, eta squared=0.038). On the other hand, we did not observe the main effects of the

hemisphere and task. For the significant main effects, we conducted a post-hoc analysis. Results showed that "hand vs. feet" classification accuracy was significantly higher than "female vs. male" classification accuracy (MD=1.566, t=3.731, p=0.001 Bonferroni-corrected). There was no other significant comparison. ROI post-hoc analysis showed that the decoding accuracy of the parietal cortex was higher than the pSTS (MD=2.227, t=8.684, p<0.001 Bonferroni-corrected) and premotor(MD=2.133, t=8.316, p<0.001 Bonferroni-corrected) decoding accuracy.

Also, a significant interaction effect of task and feature was observed. When attention is directed to a specific feature of the action, the decoding accuracy of that feature peaks. With post-hoc analysis, we discovered that for the effector task (in every ROI), the decoding accuracy for the "hand vs. feet" classification was significantly higher than both "female vs. male" accuracy (MD=2.727, t=3.956, p=0.004, Bonferroni-corrected) and "human vs. object" accuracy (MD=2.875, t=4.171, p=0.002, Bonferroni-corrected). Post-hoc analysis revealed no significant difference in feature decoding performance for actor and target tasks.

Here are the other significant interaction effects: hemi*roi*task (F=3.443, p=0.011, eta squared=0.007) and roi*task*feature(F=2.325, p=0.021, eta squared=0.012). No other significant interaction effects were found.

Chapter 4

Discussion

4.1 Discussion of the Results

In this study, we investigated how attention, as a top-down process, influences the neural representations of the AON, including the posterior pSTS, parietal, and premotor regions. Using univariate and multivariate analysis techniques, we examined how attending to specific features of action alters activation within AON nodes and whether these effects differ across regions. Our results demonstrate that all AON regions are modulated by the task being performed. Furthermore, we found that each region exhibits unique task-specific modifications, revealing distinct patterns of interaction between attention and neural processing within the AON.

Univariate results demonstrated that the AON was active during both active and passive sessions. However, we observed some differences between the activation maps of active and passive sessions. First, the activation in the active session was more extensive compared to the passive session, particularly in the parietal cortex. Additionally, activation in the premotor cortex was observed only during the active session. Consistent with the literature, adding cognitive demand resulted in extended spatial activation in the brain [55] [56]. Also, these

findings support the results of Orban et al., [29], which observed extended activation in parietal and premotor regions when participants engaged in feature-based attention tasks for actions.

We investigated the differences between tasks as the next step in the univariate analysis. The contrast maps of each task compared to the rest revealed similar activation patterns with slight differences. Behavioral results also showed no significant differences in cognitive demand between tasks, as there were no significant variations in reaction times or accuracy rates, supporting the univariate results. Considering the limitations of univariate analysis [57], we also decided to include multivariate analysis, which is more sensitive in capturing subtle neural activation patterns [58].

RSA results revealed that only the task model significantly correlated with neural RDMs. Notably, all ROIs within the AON exhibited neural patterns that aligned with the ongoing attention task. It shows that top-down attentional modulation influences every hierarchy level of the AON. Also, the correlation between the RDM of the right premotor region and the task model reached the noise ceiling level, showing that the task model alone is sufficient to explain the neural patterns in this region. Moreover, the right premotor region was the only area to reach this noise ceiling level. This result could be attributed to the premotor cortex's location within the frontal cortex and its higher hierarchical position within the AON [17]. It is plausible that top-down attentional modulation affected the premotor region more than the parietal and pSTS regions. Even though RSA revealed the presence of top-down signals influencing AON nodes, it did not uncover the feature-specific effects on the ROIs. Previous research has suggested that each ROI in the AON may decode distinct features of an action [59]. Further decoding analysis helped us to explore these features and ROI-specific top-down modulations.

Decoding accuracy values were first used for an ANOVA with hemisphere, ROI, task, and feature factors. The analysis revealed no main effect of the task. This result indicates that the task alone did not affect the decoding results, supporting the result that there was no cognitive demand difference between

tasks. Additionally, we did not observe a main effect of the hemisphere, suggesting no difference between hemispheres regarding action observation. However, there was a main effect of ROI and feature. This result suggests that some ROIs may be more successful at decoding action features, and some features may be encoded more pronounced than others, revealing unique roles of ROIs within the AON. Although there was no main effect of hemisphere, a significant hemi * ROI * task interaction indicates that for some specific ROI and task interactions, the activity patterns of hemispheres may be distinct. Similarly, the significant ROI * task * feature interaction effect demonstrates the task- and feature-specific influences on the ROIs. All these significant main and interaction effects reveal distinct neural patterns in ROIs, strongly intertwined with the given attention task and feature of the action extending previous work [28] [30] [29].

In the pSTS region, while "human vs. object" was successfully decoded under actor and target tasks, "female vs. male" and "hand vs. feet" classifications were not successful under any tasks. This distinction may have occurred due to the difference in social content of the videos in human and object conditions. In object condition, the actor pushes an object, which can be defined as a manipulation action. On the other hand, in the human condition, the actor pushes another human, creating social content. pSTS is also known to be a part of "social brain", and it encodes dynamic social cues [60] [61]. Because of the social sensitivity of the pSTS region, the neural pattern for human and object conditions may have differentiated significantly, resulting in better decoding performance.

In the parietal region, the "hand vs. feet" classification was successful under all tasks and in both hemispheres. There might be several reasons for this result. First, several studies have shown that the parietal cortex may encode effector information. For example, one study focused on reaching-grasping actions [62], showed that in parietal regions, both the grip type and the interaction between grip type and action goal can be decoded. Another reason may be that focusing on the effector leads participants to attend more to the action-performing space than when focusing on the actor or target. The space around us is represented in the parietal cortex [63] and is part of the dorsal visual system, which has a role in spatial perception [64]. This is probably why the parietal cortex can decode

the effector under all tasks.

The average decoding accuracy in the parietal cortex was significantly higher than in the pSTS and premotor regions. The parietal cortex is known to encode an action's abstract representation, helping us understand the concept of that action [65]. It is why people with brain damage in the parietal region cannot comprehend the meaning of an action, even though they perceive it [66]. Additionally, research has shown that the parietal cortex is active during action discrimination [29]. These studies reveal that the parietal cortex may encode many action features to interpret its meaning. This may explain why it was more successful in decoding features than the other ROIs.

In the premotor cortex, we observed a different decoding accuracy pattern than in the other ROIs. In the left hemisphere, "hand vs. feet" was decoded only under the effector task, and "human vs. object" classification was successful only under the target task. Similar patterns were found for the right hemisphere (see Figure 3.6). These results indicate that the premotor region did not encode the actor information but rather the effector and the target. The reason it was insensitive to the actor may be that it encodes the kinematics of an action [67] [68], and the actor does not change an action's kinematics significantly. The successful decoding for effector and target features under specific matching tasks shows that its neural patterns align highly with the ongoing task. These results may be attributable to the premotor cortex's location at a higher level of the AON hierarchy [17], resulting in top-down signals having a more substantial impact on its neural activity patterns.

Another interesting result is that decoding "female vs male" was less successful than the other features (see Results section). In the context of our investigation, action is defined as a purposeful event executed intentionally by an agent. Also, there is a dichotomy between intrinsic and extrinsic features within the concept of action, with intrinsic features constituting the action's core identity and extrinsic features being modifiable without altering its fundamental essence. In the context of our experimental framework, the target can be seen as an intrinsic feature due to its direct association with the action's purpose. For example, pushing an object

versus pushing a human carries different meanings, one involving manipulating an object's position, while the other has social implications. The effector also plays a crucial role in shaping the action's meaning and goal. Even though the same outcome is achieved, using different effectors makes us perceive them as distinct actions. For example, hitting a ball with the foot (kicking) versus the hand (slapping).

Unlike the intrinsic nature of targets and effectors, the identity of the agent doesn't fundamentally alter the action's meaning. Although there may be instances where the actor contributes to the meaning of an action, such occurrences typically depend on pre-existing expectations and familiarity with the actor. In situations like our experiment, where expectations regarding the actor are absent, the identity of the actor has minimal influence on the meaning of the action. Hence, the observed decrease in activation during the actor task, in contrast to the effector and target tasks, can be attributed to the extrinsic nature of the actor feature. Meanwhile, the intrinsic features such as the effector and the target tasks may have resulted in more pronounced activation. This discovery shows that the different features of action play different roles in the perception of action, which may hold significant importance for designing neuroscientific experiments.

4.2 Conclusion

This study investigated how feature-based attention affects the nodes of the AON. Univariate analysis showed that while watching the same action videos, adding cognitive demand extended the activity in the parietal region and involved the premotor region. RSA results showed that top-down processes modulate all AON nodes, aligning their neural patterns with current cognitive demands. Then, decoding analysis provided a more detailed picture. Brain regions within the AON operate at different hierarchical levels and encode different features or unique combinations of some features. As a result, attending to different features of an action uniquely influences the ROIs. This research demonstrates that tasks can affect multiple levels of the AON, with differential impacts on each ROI.

4.3 Limitations

It's important to acknowledge the limitations of this study. First of all, our stimuli consisted of only one action: pushing. We could not include other types of action for two reasons: First, for our experimental design, we needed to choose an action that could be performed naturally with two different effectors, significantly reducing our options. Second, the fMRI experiment was already lengthy, with each run lasting approximately 8 minutes and each video under each task presented 16 times. Adding one more type of action would have either lengthened the experiment duration or reduced the number of stimulus presentations. Although univariate analysis revealed activation in the AON, the generalizability of these results to a broader range of actions may require further investigation in future research.

Controlling for the low-level features could be considered a limitation of our study. We tried to control the movement and appearance of actors through clothing, and we chose an object that was similar in size to humans. However, due to the complex nature of the videos, it was not possible to control for all low-level features. For example, in the actor condition, the male and the female actor looked different, and in the effector condition, performing the action with feet resulted in a larger action space, and in the target condition, the human and the object looked substantially different. These differences in the low-level visual features may have helped classify these features in the decoding analysis. However, since our study did not focus on early visual areas of the brain, we cannot definitively conclude that these differences significantly influenced the results. Our RSA results did not reveal any significant correlations between the visual model and neural RDMs in any ROI.

Additionally, our research did not include eye-tracking measures to monitor participants' gaze movements during the experiment. Although participants were instructed to maintain fixation on a central cross on the screen, our ability to verify their adherence to this instruction was limited. Eye movements can evoke brain activity and introduce a source of variability our study did not control for

[69]. This potential confound should be considered when interpreting the results.

4.4 Future Directions

First, there is a growing emphasis on employing more ecologically valid stimuli in neuroscience. Using artificial stimuli that do not reflect real-world scenarios can raise concerns regarding the generalizability of research findings. Studies incorporating more naturalistic stimuli, such as those employed in the current study, and even those involving real actors as observed in recent work [70], are gaining importance. This research path can result in insights that more accurately reflect the brain's functioning in real life, advancing our understanding of cognitive processes [71].

Second, our research demonstrated that different tasks can distinctly influence activity patterns within brain regions. In neuroscience research, tasks are sometimes used to engage participants' attention, independent of the study's primary focus. For example, n-back tasks might be used in a color perception task. However, researchers should consider the effects of these tasks more carefully, as they may activate unrelated brain regions. This introduces variability in the study results. Future research should investigate these tasks and the resulting top-down modulations. Additionally, this study highlighted that the brain operates as a network, and it is not always possible to separate top-down and bottom-up effects. When designing computational models of action perception, incorporating top-down signals is crucial for a more comprehensive understanding of neural mechanisms and interactions between brain regions.

With the rise and growing influence of AI models and their integration into daily life, accurately detecting and defining actions is becoming increasingly important. Image recognition has already seen significant advancements, and action recognition is the next major step, building upon existing research. Algorithms capable of detecting human actions offer many potential applications. For example, advanced search algorithms employed in drones could enhance rescue missions

after disasters or be used to detect unusual behaviors like theft and fights to improve city safety. Also, action recognition is critical in developing autonomous vehicles and robotics. Designing computational models of action perception has the potential to inspire and directly contribute to the field of AI, as has occurred numerous times in the past. Future studies on real-time action perception models will undoubtedly contribute to these valuable outcomes.

Bibliography

[1] S. Caspers, K. Zilles, A. R. Laird, and S. B. Eickhoff, "Ale meta-analysis of action observation and imitation in the human brain," *Neuroimage*, vol. 50, no. 3, pp. 1148–1167, 2010.

[2] K. Amunts, A. Schleicher, U. Bürgel, H. Mohlberg, H. B. Uylings, and K. Zilles, "Broca's region revisited: cytoarchitecture and intersubject variability," *Journal of comparative neurology*, vol. 412, no. 2, pp. 319–341, 1999.

[3] S. Geyer, "The microstructural border between the motor and the cognitive domain in the human cerebral cortex," 2012.

[4] C. Grefkes, S. Geyer, T. Schormann, P. Roland, and K. Zilles, "Human somatosensory area 2: observer-independent cytoarchitectonic mapping, interindividual variability, and population map," *Neuroimage*, vol. 14, no. 3, pp. 617–631, 2001.

[5] F. Scheperjans, K. Hermann, S. B. Eickhoff, K. Amunts, A. Schleicher, and K. Zilles, "Observer-independent cytoarchitectonic mapping of the human superior parietal cortex," *Cerebral Cortex*, vol. 18, no. 4, pp. 846–867, 2008.

[6] S. Caspers, S. Geyer, A. Schleicher, H. Mohlberg, K. Amunts, and K. Zilles, "The human inferior parietal cortex: cytoarchitectonic parcellation and interindividual variability," *Neuroimage*, vol. 33, no. 2, pp. 430–448, 2006.

[7] S. Caspers, S. B. Eickhoff, S. Geyer, F. Scheperjans, H. Mohlberg, K. Zilles, and K. Amunts, "The human inferior parietal lobule in stereotaxic space," *Brain Structure and Function*, vol. 212, pp. 481–495, 2008.

[8] A. Malikovic, K. Amunts, A. Schleicher, H. Mohlberg, S. B. Eickhoff, M. Wilms, N. Palomero-Gallagher, E. Armstrong, and K. Zilles, "Cytoarchitectonic analysis of the human extrastriate cortex in the region of v5/mt+: a probabilistic, stereotaxic map of area hoc5," *Cerebral cortex*, vol. 17, no. 3, pp. 562–574, 2007.

[9] D. H. Hubel and T. N. Wiesel, "Receptive fields and functional architecture of monkey striate cortex," *The Journal of physiology*, vol. 195, no. 1, pp. 215–243, 1968.

[10] L. C. Sincich and J. C. Horton, "The circuitry of v1 and v2: integration of color, form, and motion," *Annu. Rev. Neurosci.*, vol. 28, pp. 303–326, 2005.

[11] R. Gattass, J. Soares, and B. Lima, "Visual maps and visual perception," *Journal of Ophthalmology and Eye Care*, vol. 3, no. 1, p. 101, 2021.

[12] M. A. Goodale and A. D. Milner, "Separate visual pathways for perception and action," *Trends in neurosciences*, vol. 15, no. 1, pp. 20–25, 1992.

[13] L. L. Chao and A. Martin, "Representation of manipulable man-made objects in the dorsal stream," *Neuroimage*, vol. 12, no. 4, pp. 478–484, 2000.

[14] K. Krug, N. Cicmil, A. J. Parker, and B. G. Cumming, "A causal role for v5/mt neurons coding motion-disparity conjunctions in resolving perceptual ambiguity," *Current Biology*, vol. 23, no. 15, pp. 1454–1459, 2013.

[15] P. Pietrini, M. L. Furey, E. Ricciardi, M. I. Gobbini, W.-H. C. Wu, L. Cohen, M. Guazzelli, and J. V. Haxby, "Beyond sensory images: Object-based representation in the human ventral pathway," *Proceedings of the National Academy of Sciences*, vol. 101, no. 15, pp. 5658–5663, 2004.

[16] A. P. Saygin, "Superior temporal and premotor brain areas necessary for biological motion perception," *Brain*, vol. 130, no. 9, pp. 2452–2461, 2007.

[17] K. Nelissen, E. Borra, M. Gerbella, S. Rozzi, G. Luppino, W. Vanduffel, G. Rizzolatti, and G. A. Orban, "Action observation circuits in the macaque monkey cortex," *Journal of Neuroscience*, vol. 31, no. 10, pp. 3743–3756, 2011.

[18] K. Kay, K. Bonnen, R. N. Denison, M. J. Arcaro, and D. L. Barack, "Tasks and their role in visual neuroscience," *Neuron*, 2023.

[19] M. A. Giese and T. Poggio, "Neural mechanisms for the recognition of biological movements," *Nature Reviews Neuroscience*, vol. 4, no. 3, pp. 179–192, 2003.

[20] J. M. Kilner, K. J. Friston, and C. D. Frith, "Predictive coding: an account of the mirror neuron system," *Cognitive processing*, vol. 8, pp. 159–166, 2007.

[21] B. A. Urgen and A. P. Saygin, "Predictive processing account of action perception: Evidence from effective connectivity in the action observation network," *Cortex*, vol. 128, pp. 132–142, 2020.

[22] A. Borji and L. Itti, "State-of-the-art in visual attention modeling," *IEEE transactions on pattern analysis and machine intelligence*, vol. 35, no. 1, pp. 185–207, 2012.

[23] M. Carrasco, "Visual attention: The past 25 years," *Vision research*, vol. 51, no. 13, pp. 1484–1525, 2011.

[24] S. Yantis and J. T. Serences, "Cortical mechanisms of space-based and object-based attentional control," *Current opinion in neurobiology*, vol. 13, no. 2, pp. 187–193, 2003.

[25] M. R. Cohen and J. H. Maunsell, "Attention improves performance primarily by reducing interneuronal correlations," *Nature neuroscience*, vol. 12, no. 12, pp. 1594–1600, 2009.

[26] J. H. Maunsell and S. Treue, "Feature-based attention in visual cortex," *Trends in neurosciences*, vol. 29, no. 6, pp. 317–322, 2006.

[27] S. Treue, "Visual attention: the where, what, how and why of saliency," *Current opinion in neurobiology*, vol. 13, no. 4, pp. 428–432, 2003.

[28] D. A. Stehr, X. Zhou, M. Tisby, P. T. Hwu, J. A. Pyles, and E. D. Grossman, "Top-down attention guidance shapes action encoding in the psts," *Cerebral Cortex*, vol. 31, no. 7, pp. 3522–3535, 2021.

[29] G. A. Orban, S. Ferri, and A. Platonov, "The role of putative human anterior intraparietal sulcus area in observed manipulative action discrimination," *Brain and Behavior*, vol. 9, no. 3, p. e01226, 2019.

[30] M. Shahdloo, E. Çelik, B. A. Urgen, J. L. Gallant, and T. Çukur, "Task-dependent warping of semantic representations during search for visual action categories," *Journal of Neuroscience*, vol. 42, no. 35, pp. 6782–6799, 2022.

[31] O. Esteban, C. J. Markiewicz, R. W. Blair, C. A. Moodie, A. I. Isik, A. Erramuzpe, J. D. Kent, M. Goncalves, E. DuPre, M. Snyder, *et al.*, "fmriprep: a robust preprocessing pipeline for functional mri," *Nature methods*, vol. 16, no. 1, pp. 111–116, 2019.

[32] K. Gorgolewski, C. D. Burns, C. Madison, D. Clark, Y. O. Halchenko, M. L. Waskom, and S. S. Ghosh, "Nipype: a flexible, lightweight and extensible neuroimaging data processing framework in python," *Frontiers in neuroinformatics*, vol. 5, p. 13, 2011.

[33] K. J. Gorgolewski, O. Esteban, D. G. Ellis, M. P. Notter, E. Ziegler, H. Johnson, C. Hamalainen, B. Yvernault, C. Burns, A. Manhães-Savio, D. Jarecka, C. J. Markiewicz, T. Salo, D. Clark, M. Waskom, J. Wong, M. Modat, B. E. Dewey, M. G. Clark, M. Dayan, F. Loney, C. Madison, A. Gramfort, A. Keshavan, S. Berleant, B. Pinsard, M. Goncalves, D. Clark, B. Cipollini, G. Varoquaux, D. Wassermann, A. Rokem, Y. O. Halchenko, J. Forbes, B. Moloney, I. B. Malone, M. Hanke, D. Mordom, C. Buchanan, W. M. Pauli, J. M. Huntenburg, C. Horea, Y. Schwartz, R. Tungaraza, S. Iqbal, J. Kleesiek, S. Sikka, C. Frohlich, J. Kent, M. Perez-Guevara, A. Watanabe, D. Welch, C. Cumba, D. Ginsburg, A. Eshaghi, E. Kastman, S. Bougacha, R. Blair, B. Acland, A. Gillman, A. Schaefer, B. N. Nichols, S. Giavasis, D. Erickson, C. Correa, A. Ghayoor, R. Küttner, C. Haselgrove, D. Zhou, R. C. Craddock, D. Haehn, L. Lampe, J. Millman, J. Lai, M. Renfro, S. Liu, J. Stadler, T. Glatard, A. E. Kahn, X.-Z. Kong, W. Triplett, A. Park, C. McDermottroe, M. Hallquist, R. Poldrack,

L. N. Perkins, M. Noel, S. Gerhard, J. Salvatore, F. Mertz, W. Broderick, S. Inati, O. Hinds, M. Brett, J. Durnez, A. Tambini, S. Rothmei, S. K. Andberg, G. Cooper, A. Marina, A. Mattfeld, S. Urchs, P. Sharp, K. Matsubara, D. Geisler, B. Cheung, A. Floren, T. Nickson, N. Pannetier, A. Weinstein, M. Dubois, J. Arias, C. Tarbert, K. Schlamp, K. Jordan, F. Liem, V. Saase, R. Harms, R. Khanuja, K. Podranski, G. Flandin, D. Papadopoulos Orfanos, I. Schwabacher, D. McNamee, M. Falkiewicz, J. Pellman, J. Linkersdörfer, J. Varada, F. Pérez-García, A. Davison, D. Shachnev, and S. Ghosh, "Nipype: a flexible, lightweight and extensible neuroimaging data processing framework in python. 0.13.1."

[34] A. M. Dale, B. Fischl, and M. I. Sereno, "Cortical surface-based analysis: I. segmentation and surface reconstruction," *Neuroimage*, vol. 9, no. 2, pp. 179–194, 1999.

[35] A. Klein, S. S. Ghosh, F. S. Bao, J. Giard, Y. Häme, E. Stavsky, N. Lee, B. Rossa, M. Reuter, E. Chaibub Neto, *et al.*, "Mindboggling morphometry of human brains," *PLoS computational biology*, vol. 13, no. 2, p. e1005350, 2017.

[36] V. S. Fonov, A. C. Evans, R. C. McKinstry, C. R. Almli, and D. Collins, "Unbiased nonlinear average age-appropriate brain templates from birth to adulthood," *NeuroImage*, vol. 47, p. S102, 2009.

[37] B. B. Avants, C. L. Epstein, M. Grossman, and J. C. Gee, "Symmetric diffeomorphic image registration with cross-correlation: evaluating automated labeling of elderly and neurodegenerative brain," *Medical image analysis*, vol. 12, no. 1, pp. 26–41, 2008.

[38] Y. Zhang, M. Brady, and S. Smith, "Segmentation of brain mr images through a hidden markov random field model and the expectation-maximization algorithm," *IEEE transactions on medical imaging*, vol. 20, no. 1, pp. 45–57, 2001.

[39] R. W. Cox, "Afni: software for analysis and visualization of functional magnetic resonance neuroimages," *Computers and Biomedical research*, vol. 29, no. 3, pp. 162–173, 1996.

[40] M. Jenkinson, P. Bannister, M. Brady, and S. Smith, "Improved optimization for the robust and accurate linear registration and motion correction of brain images," *Neuroimage*, vol. 17, no. 2, pp. 825–841, 2002.

[41] D. N. Greve and B. Fischl, "Accurate and robust brain image alignment using boundary-based registration," *Neuroimage*, vol. 48, no. 1, pp. 63–72, 2009.

[42] Y. Behzadi, K. Restom, J. Liau, and T. T. Liu, "A component based noise correction method (compcor) for bold and perfusion based fmri," *Neuroimage*, vol. 37, no. 1, pp. 90–101, 2007.

[43] J. D. Power, A. Mitra, T. O. Laumann, A. Z. Snyder, B. L. Schlaggar, and S. E. Petersen, "Methods to detect, characterize, and remove motion artifact in resting state fmri," *Neuroimage*, vol. 84, pp. 320–341, 2014.

[44] A. Abraham, F. Pedregosa, M. Eickenberg, P. Gervais, A. Mueller, J. Kossaifi, A. Gramfort, B. Thirion, and G. Varoquaux, "Machine learning for neuroimaging with scikit-learn," *Frontiers in neuroinformatics*, vol. 8, p. 14, 2014.

[45] N. Kriegeskorte, M. Mur, and P. A. Bandettini, "Representational similarity analysis-connecting the branches of systems neuroscience," *Frontiers in systems neuroscience*, vol. 2, p. 249, 2008.

[46] J. Diedrichsen and N. Kriegeskorte, "Representational models: A common framework for understanding encoding, pattern-component, and representational-similarity analysis," *PLoS computational biology*, vol. 13, no. 4, p. e1005508, 2017.

[47] H. Nili, C. Wingfield, A. Walther, L. Su, W. Marslen-Wilson, and N. Kriegeskorte, "A toolbox for representational similarity analysis," *PLoS computational biology*, vol. 10, no. 4, p. e1003553, 2014.

[48] J. V. Haxby, M. I. Gobbini, M. L. Furey, A. Ishai, J. L. Schouten, and P. Pietrini, "Distributed and overlapping representations of faces and objects in ventral temporal cortex," *Science*, vol. 293, no. 5539, pp. 2425–2430, 2001.

[49] J.-D. Haynes and G. Rees, "Decoding mental states from brain activity in humans," *Nature reviews neuroscience*, vol. 7, no. 7, pp. 523–534, 2006.

[50] M. N. Hebart, K. Görgen, and J.-D. Haynes, "The decoding toolbox (tdt): a versatile software package for multivariate analyses of functional imaging data," *Frontiers in neuroinformatics*, vol. 8, p. 88, 2015.

[51] C.-C. Chang and C.-J. Lin, "Libsvm: a library for support vector machines," *ACM transactions on intelligent systems and technology (TIST)*, vol. 2, no. 3, pp. 1–27, 2011.

[52] G. A. Orban, "Functional definitions of parietal areas in human and non-human primates," *Proceedings of the Royal Society B: Biological Sciences*, vol. 283, no. 1828, p. 20160118, 2016.

[53] S. Ferri, G. Rizzolatti, and G. A. Orban, "The organization of the posterior parietal cortex devoted to upper limb actions: An fmri study," *Human brain mapping*, vol. 36, no. 10, pp. 3845–3866, 2015.

[54] E. T. Rolls, C.-C. Huang, C.-P. Lin, J. Feng, and M. Joliot, "Automated anatomical labelling atlas 3," *Neuroimage*, vol. 206, p. 116189, 2020.

[55] J. Coull and C. Frith, "Differential activation of right superior parietal cortex and intraparietal sulcus by spatial and nonspatial attention," *Neuroimage*, vol. 8, no. 2, pp. 176–187, 1998.

[56] M. Corbetta and G. L. Shulman, "Control of goal-directed and stimulus-driven attention in the brain," *Nature reviews neuroscience*, vol. 3, no. 3, pp. 201–215, 2002.

[57] G. Chen, N. E. Adleman, Z. S. Saad, E. Leibenluft, and R. W. Cox, "Applications of multivariate modeling to neuroimaging group analysis: a comprehensive alternative to univariate general linear model," *Neuroimage*, vol. 99, pp. 571–588, 2014.

[58] J.-D. Haynes, "A primer on pattern-based approaches to fmri: principles, pitfalls, and perspectives," *Neuron*, vol. 87, no. 2, pp. 257–270, 2015.

[59] B. A. Urgen, S. Pehlivan, and A. P. Saygin, "Distinct representations in occipito-temporal, parietal, and premotor cortex during action perception revealed by fmri and computational modeling," *Neuropsychologia*, vol. 127, pp. 35–47, 2019.

[60] S. Dasgupta, S. C. Tyler, J. Wicks, R. Srinivasan, and E. D. Grossman, "Network connectivity of the right sts in three social perception localizers," *Journal of Cognitive Neuroscience*, vol. 29, no. 2, pp. 221–234, 2017.

[61] J. M. Lahnakoski, E. Glerean, J. Salmi, I. P. Jääskeläinen, M. Sams, R. Hari, and L. Nummenmaa, "Naturalistic fmri mapping reveals superior temporal sulcus as the hub for the distributed brain network for social perception," *Frontiers in human neuroscience*, vol. 6, p. 233, 2012.

[62] A. Errante, S. Ziccarelli, G. P. Mingolla, and L. Fogassi, "Decoding grip type and action goal during the observation of reaching-grasping actions: A multivariate fmri study," *NeuroImage*, vol. 243, p. 118511, 2021.

[63] C. L. Colby and M. E. Goldberg, "Space and attention in parietal cortex," *Annual review of neuroscience*, vol. 22, no. 1, pp. 319–349, 1999.

[64] M. Mishkin, L. G. Ungerleider, and K. A. Macko, "Object vision and spatial vision: two cortical pathways," *Trends in neurosciences*, vol. 6, pp. 414–417, 1983.

[65] J. Gottlieb, "From thought to action: the parietal cortex as a bridge between perception, action, and cognition," *Neuron*, vol. 53, no. 1, pp. 9–16, 2007.

[66] E. Binder, A. Dovern, M. D. Hesse, M. Ebke, H. Karbe, J. Saliger, G. R. Fink, and P. H. Weiss, "Lesion evidence for a human mirror neuron system," *Cortex*, vol. 90, pp. 125–137, 2017.

[67] F. Binkofski and G. Buccino, "The role of ventral premotor cortex in action execution and action understanding," *Journal of Physiology-Paris*, vol. 99, no. 4-6, pp. 396–405, 2006.

[68] K. Takahashi, M. D. Best, N. Huh, K. A. Brown, A. A. Tobaa, and N. G. Hatsopoulos, "Encoding of both reaching and grasping kinematics in dorsal and ventral premotor cortices," *Journal of Neuroscience*, vol. 37, no. 7, pp. 1733–1746, 2017.

[69] A. C. Schütz, D. I. Braun, and K. R. Gegenfurtner, "Eye movements and perception: A selective review," *Journal of vision*, vol. 11, no. 5, pp. 9–9, 2011.

[70] T. N. Pekçetin, Ş. Evsen, S. Pekçetin, C. Acarturk, and B. A. Urgen, "A naturalistic setup for presenting real people and live actions in experimental psychology and cognitive neuroscience studies," *JoVE (Journal of Visualized Experiments)*, no. 198, p. e65436, 2023.

[71] A. Maselli, J. Gordon, M. Eluchans, G. L. Lancia, T. Thiery, R. Moretti, P. Cisek, and G. Pezzulo, "Beyond simple laboratory studies: developing sophisticated models to study rich behavior," *Physics of Life Reviews*, 2023.

Appendix A

Code

For the codes and videos used for this study, check out the author's GitHub profile: https://github.com/aslieroglu

Appendix B

Permissions

ELSEVIER LICENSE
TERMS AND CONDITIONS

Jun 15, 2024

This Agreement between Aslı Eroğlu ("You") and Elsevier ("Elsevier") consists of your license details and the terms and conditions provided by Elsevier and Copyright Clearance Center.

License Number	5810391453263
License date	Jun 15, 2024
Licensed Content Publisher	Elsevier
Licensed Content Publication	NeuroImage
Licensed Content Title	ALE meta-analysis of action observation and imitation in the human brain
Licensed Content Author	Svenja Caspers,Karl Zilles,Angela R. Laird,Simon B. Eickhoff
Licensed Content Date	Apr 15, 2010
Licensed Content Volume	50
Licensed Content Issue	3
Licensed Content Pages	20
Start Page	1148
End Page	1167
Type of Use	reuse in a thesis/dissertation

Portion	figures/tables/illustrations
Number of figures/tables/illustrations	1
Format	both print and electronic
Are you the author of this Elsevier article?	No
Will you be translating?	No
Title of new work	TOP-DOWN EFFECTS OF ATTENTION ON THE ACTION OBSERVATION NETWORK
Institution name	Bilkent University
Expected presentation date	Jul 2024
Order reference number	seven
Portions	Figure 1
The Requesting Person / Organization to Appear on the License	Aslı Eroğlu
Requestor Location	Aslı Eroğlu Bilkent University Main Campus Ankara, 06800 Turkey Attn: Aslı Eroğlu
Publisher Tax ID	GB 494 6272 12
Total	0.00 USD
Terms and Conditions	

INTRODUCTION

1. The publisher for this copyrighted material is Elsevier. By clicking "accept" in connection with completing this licensing transaction, you agree that the following terms and conditions apply to this transaction (along with the Billing and Payment terms and conditions established by Copyright Clearance Center, Inc. ("CCC"), at the time that you opened your RightsLink account and that are available at any time at https://myaccount.copyright.com).

GENERAL TERMS

2. Elsevier hereby grants you permission to reproduce the aforementioned material subject to the terms and conditions indicated.

3. Acknowledgement: If any part of the material to be used (for example, figures) has appeared in our publication with credit or acknowledgement to another source, permission must also be sought from that source. If such permission is not obtained then that material may not be included in your publication/copies. Suitable acknowledgement to the source must be made, either as a footnote or in a reference list at the end of your publication, as follows:

"Reprinted from Publication title, Vol /edition number, Author(s), Title of article / title of chapter, Pages No., Copyright (Year), with permission from Elsevier [OR APPLICABLE SOCIETY COPYRIGHT OWNER]." Also Lancet special credit - "Reprinted from The Lancet, Vol. number, Author(s), Title of article, Pages No., Copyright (Year), with permission from Elsevier."

4. Reproduction of this material is confined to the purpose and/or media for which permission is hereby given. The material may not be reproduced or used in any other way, including use in combination with an artificial intelligence tool (including to train an algorithm, test, process, analyse, generate output and/or develop any form of artificial intelligence tool), or to create any derivative work and/or service (including resulting from the use of artificial intelligence tools).

5. Altering/Modifying Material: Not Permitted. However figures and illustrations may be altered/adapted minimally to serve your work. Any other abbreviations, additions, deletions and/or any other alterations shall be made only with prior written authorization of Elsevier Ltd. (Please contact Elsevier's permissions helpdesk here). No modifications can be made to any Lancet figures/tables and they must be reproduced in full.

6. If the permission fee for the requested use of our material is waived in this instance, please be advised that your future requests for Elsevier materials may attract a fee.

7. Reservation of Rights: Publisher reserves all rights not specifically granted in the combination of (i) the license details provided by you and accepted in the course of this licensing transaction, (ii) these terms and conditions and (iii) CCC's Billing and Payment terms and conditions.

8. License Contingent Upon Payment: While you may exercise the rights licensed immediately upon issuance of the license at the end of the licensing process for the transaction, provided that you have disclosed complete and accurate details of your proposed use, no license is finally effective unless and until full payment is received from you (either by publisher or by CCC) as provided in CCC's Billing and Payment terms and conditions. If full payment is not received on a timely basis, then any license preliminarily granted shall be deemed automatically revoked and shall be void as if never granted. Further, in the event that you breach any of these terms and conditions or any of CCC's Billing and Payment terms and conditions, the license is automatically revoked and shall be void as if never granted. Use of materials as described in a revoked license, as well as any use of the materials beyond the scope of an unrevoked license, may constitute copyright infringement and publisher reserves the right to take any and all action to protect its copyright in the materials.

9. Warranties: Publisher makes no representations or warranties with respect to the licensed material.

10. Indemnity: You hereby indemnify and agree to hold harmless publisher and CCC, and their respective officers, directors, employees and agents, from and against any and all claims arising out of your use of the licensed material other than as specifically authorized pursuant to this license.

11. No Transfer of License: This license is personal to you and may not be sublicensed, assigned, or transferred by you to any other person without publisher's written permission.

12. No Amendment Except in Writing: This license may not be amended except in a writing signed by both parties (or, in the case of publisher, by CCC on publisher's behalf).

13. Objection to Contrary Terms: Publisher hereby objects to any terms contained in any purchase order, acknowledgment, check endorsement or other writing prepared by you, which terms are inconsistent with these terms and conditions or CCC's Billing and Payment terms and conditions. These terms and conditions, together with CCC's Billing and Payment terms and conditions (which are incorporated herein), comprise the entire agreement between you and publisher (and CCC) concerning this licensing transaction. In the event of any conflict between your obligations established by these terms and conditions and those established by CCC's Billing and Payment terms and conditions, these terms and conditions shall control.

14. Revocation: Elsevier or Copyright Clearance Center may deny the permissions described in this License at their sole discretion, for any reason or no reason, with a full refund payable to you. Notice of such denial will be made using the contact information provided by you. Failure to receive such notice will not alter or invalidate the denial. In no event will Elsevier or Copyright Clearance Center be responsible or liable for any costs, expenses or damage incurred by you as a result of a denial of your permission request, other than a refund of the amount(s) paid by you to Elsevier and/or Copyright Clearance Center for denied permissions.

LIMITED LICENSE

The following terms and conditions apply only to specific license types:

15. **Translation**: This permission is granted for non-exclusive world **English** rights only unless your license was granted for translation rights. If you licensed translation rights you may only translate this content into the languages you requested. A professional translator must perform all translations and reproduce the content word for word preserving the integrity of the article.

16. **Posting licensed content on any Website**: The following terms and conditions apply as follows: Licensing material from an Elsevier journal: All content posted to the web site must maintain the copyright information line on the bottom of each image; A hyper-text must be included to the Homepage of the journal from which you are licensing at http://www.sciencedirect.com/science/journal/xxxxx or the Elsevier homepage for books at http://www.elsevier.com; Central Storage: This license does not include permission for a scanned version of the material to be stored in a central repository such as that provided by Heron/XanEdu.

Licensing material from an Elsevier book: A hyper-text link must be included to the Elsevier homepage at http://www.elsevier.com . All content posted to the web site must maintain the copyright information line on the bottom of each image.

Posting licensed content on Electronic reserve: In addition to the above the following clauses are applicable: The web site must be password-protected and made available only

to bona fide students registered on a relevant course. This permission is granted for 1 year only. You may obtain a new license for future website posting.

17. **For journal authors:** the following clauses are applicable in addition to the above:

Preprints:

A preprint is an author's own write-up of research results and analysis, it has not been peer-reviewed, nor has it had any other value added to it by a publisher (such as formatting, copyright, technical enhancement etc.).

Authors can share their preprints anywhere at any time. Preprints should not be added to or enhanced in any way in order to appear more like, or to substitute for, the final versions of articles however authors can update their preprints on arXiv or RePEc with their Accepted Author Manuscript (see below).

If accepted for publication, we encourage authors to link from the preprint to their formal publication via its DOI. Millions of researchers have access to the formal publications on ScienceDirect, and so links will help users to find, access, cite and use the best available version. Please note that Cell Press, The Lancet and some society-owned have different preprint policies. Information on these policies is available on the journal homepage.

Accepted Author Manuscripts: An accepted author manuscript is the manuscript of an article that has been accepted for publication and which typically includes author-incorporated changes suggested during submission, peer review and editor-author communications.

Authors can share their accepted author manuscript:

- immediately
    - via their non-commercial person homepage or blog
    - by updating a preprint in arXiv or RePEc with the accepted manuscript
    - via their research institute or institutional repository for internal institutional uses or as part of an invitation-only research collaboration work-group
    - directly by providing copies to their students or to research collaborators for their personal use
    - for private scholarly sharing as part of an invitation-only work group on commercial sites with which Elsevier has an agreement
- After the embargo period
    - via non-commercial hosting platforms such as their institutional repository
    - via commercial sites with which Elsevier has an agreement

In all cases accepted manuscripts should:

- link to the formal publication via its DOI
- bear a CC-BY-NC-ND license - this is easy to do
- if aggregated with other manuscripts, for example in a repository or other site, be shared in alignment with our hosting policy not be added to or enhanced in any way to appear more like, or to substitute for, the published journal article.

Published journal article (JPA): A published journal article (PJA) is the definitive final record of published research that appears or will appear in the journal and embodies all value-adding publishing activities including peer review co-ordination, copy-editing, formatting, (if relevant) pagination and online enrichment.

Policies for sharing publishing journal articles differ for subscription and gold open access articles:

Subscription Articles: If you are an author, please share a link to your article rather than the full-text. Millions of researchers have access to the formal publications on ScienceDirect, and so links will help your users to find, access, cite, and use the best available version.

Theses and dissertations which contain embedded PJAs as part of the formal submission can be posted publicly by the awarding institution with DOI links back to the formal publications on ScienceDirect.

If you are affiliated with a library that subscribes to ScienceDirect you have additional private sharing rights for others' research accessed under that agreement. This includes use for classroom teaching and internal training at the institution (including use in course packs and courseware programs), and inclusion of the article for grant funding purposes.

Gold Open Access Articles: May be shared according to the author-selected end-user license and should contain a CrossMark logo, the end user license, and a DOI link to the formal publication on ScienceDirect.

Please refer to Elsevier's posting policy for further information.

18. **For book authors** the following clauses are applicable in addition to the above: Authors are permitted to place a brief summary of their work online only. You are not allowed to download and post the published electronic version of your chapter, nor may you scan the printed edition to create an electronic version. **Posting to a repository:** Authors are permitted to post a summary of their chapter only in their institution's repository.

19. **Thesis/Dissertation**: If your license is for use in a thesis/dissertation your thesis may be submitted to your institution in either print or electronic form. Should your thesis be published commercially, please reapply for permission. These requirements include permission for the Library and Archives of Canada to supply single copies, on demand, of the complete thesis and include permission for Proquest/UMI to supply single copies, on demand, of the complete thesis. Should your thesis be published commercially, please reapply for permission. Theses and dissertations which contain embedded PJAs as part of the formal submission can be posted publicly by the awarding institution with DOI links back to the formal publications on ScienceDirect.

Elsevier Open Access Terms and Conditions

You can publish open access with Elsevier in hundreds of open access journals or in nearly 2000 established subscription journals that support open access publishing. Permitted third party re-use of these open access articles is defined by the author's choice of Creative Commons user license. See our open access license policy for more information.

Terms & Conditions applicable to all Open Access articles published with Elsevier:

Any reuse of the article must not represent the author as endorsing the adaptation of the article nor should the article be modified in such a way as to damage the author's honour or reputation. If any changes have been made, such changes must be clearly indicated.

The author(s) must be appropriately credited and we ask that you include the end user license and a DOI link to the formal publication on ScienceDirect.

If any part of the material to be used (for example, figures) has appeared in our publication with credit or acknowledgement to another source it is the responsibility of the

user to ensure their reuse complies with the terms and conditions determined by the rights holder.

Additional Terms & Conditions applicable to each Creative Commons user license:

CC BY: The CC-BY license allows users to copy, to create extracts, abstracts and new works from the Article, to alter and revise the Article and to make commercial use of the Article (including reuse and/or resale of the Article by commercial entities), provided the user gives appropriate credit (with a link to the formal publication through the relevant DOI), provides a link to the license, indicates if changes were made and the licensor is not represented as endorsing the use made of the work. The full details of the license are available at http://creativecommons.org/licenses/by/4.0.

CC BY NC SA: The CC BY-NC-SA license allows users to copy, to create extracts, abstracts and new works from the Article, to alter and revise the Article, provided this is not done for commercial purposes, and that the user gives appropriate credit (with a link to the formal publication through the relevant DOI), provides a link to the license, indicates if changes were made and the licensor is not represented as endorsing the use made of the work. Further, any new works must be made available on the same conditions. The full details of the license are available at http://creativecommons.org/licenses/by-nc-sa/4.0.

CC BY NC ND: The CC BY-NC-ND license allows users to copy and distribute the Article, provided this is not done for commercial purposes and further does not permit distribution of the Article if it is changed or edited in any way, and provided the user gives appropriate credit (with a link to the formal publication through the relevant DOI), provides a link to the license, and that the licensor is not represented as endorsing the use made of the work. The full details of the license are available at http://creativecommons.org/licenses/by-nc-nd/4.0. Any commercial reuse of Open Access articles published with a CC BY NC SA or CC BY NC ND license requires permission from Elsevier and will be subject to a fee.

Commercial reuse includes:

- Associating advertising with the full text of the Article
- Charging fees for document delivery or access
- Article aggregation
- Systematic distribution via e-mail lists or share buttons

Posting or linking by commercial companies for use by customers of those companies.

20. **Other Conditions**:

v1.10

Questions? customercare@copyright.com.